Global evaluation of nutrient enabled version land surface model ORCHIDEE-CNP v1.2 (r5986)

Yan Sun[1], Daniel S Goll[1,2], Jinfeng Chang[3], Philippe Ciais[1], Betrand Guenet[1,4], Julian Helfenstein[5], Yuanyuan Huang[1,6], Ronny Lauerwald[1,7], Fabienne Maignan[1], Victoria Naipal[1,8], Yilong Wang[1,9], Hui Yang[1], Haicheng Zhang[1,7]

[1]Laboratoire des Sciences du Climat et de 1'Environnement/IPSL, CEA-CNRS-UVSQ, Université Paris-Saclay, Gif sur Yvette, 91191, France.
[2] Department of Geography, University of Augsburg, Augsburg, Germany
[3] Ecosystems Services and Management Program, International Institute for Applied Systems Analysis (IIASA), Schlossplatz 1, A-2361 Laxenburg, Austria
[4] Laboratoire de Géologie, UMR 8538, Ecole Normale Supérieure, PSL Research University, CNRS, Paris, France
[5]Agroecology and Environment, Agroscope, Reckenholzstrasse 191, 8046 Zurich, Switzerland
[6] CSIRO Oceans and Atmosphere, Aspendale 3195, Australia
[7] Department Geoscience, Environment & Society, Universite libre de Bruxelles, 1050 Bruxelles, Belgium
[8] Department of Geography, Ludwig-Maximilian University, Munich, Germany
[9] Key Laboratory of Land Surface Pattern and Simulation, Institute of Geographical Sciences and Natural Resources Research, Chinese Academy of Sciences, Beijing, China

Correspondence to: Yan SUN (ysun@lsce.ipsl.fr); Daniel S. Goll (dsgoll123@gmail.com)

Abstract. The availability of phosphorus (P) and nitrogen (N) constrain the ability of ecosystems to use resources such as light, water and carbon. In turn, nutrients impact the distribution of productivity, ecosystem carbon turnovers and their net exchange of CO_2 with the atmosphere in response to variation of environmental conditions both in space and in time. In this study, we evaluated the performance of the global version of the land surface model ORCHIDEE-CNP (v1.2) which explicitly simulates N and P biogeochemistry in terrestrial ecosystems coupled with carbon, water and energy transfers. We used data from remote-sensing, ground-based measurement networks and ecological databases. Components of the N and P cycle at different levels of aggregation (from local to global) are in good agreement with data-driven estimates. When integrated for the period 1850 to 2017 forced with variable climate, rising CO_2 and land use change, we show that ORCHIDEE-CNP underestimates the land carbon sink in the North Hemisphere (NH) during the recent decades, despite an a priori realistic GPP response to rising CO_2. This result suggests either that other processes than CO_2 fertilization which are omitted in ORCHIDEE-CNP, such as changes in biomass turnover, are predominant drivers of the northern land sink, and/or that the model parameterizations produce too strict emerging nutrient limitations on biomass growth in northern areas. In line with the latter, we identified biases in the simulated large-scale patterns of leaf and soil stoichiometry and plant P use efficiency pointing towards a too severe P limitations towards the poles. Based on our analysis of ecosystem resource use efficiencies and nutrient cycling, we propose ways to address the model biases by giving priority to better representing processes of soil organic P mineralization and soil inorganic P transformation, followed by refining the biomass

production efficiency under increasing atmospheric CO_2, phenology dynamics and canopy light absorption.

1 Introduction

Nitrogen (N) and phosphorus (P) are key macronutrients that control metabolic processes and plant growth and constrain ecosystem-level productivity (Elser et al., 2007; Norby et al., 2010; Cleveland et al., 2013). The amount and stability of soil carbon (C) stock is also affected by N and P through their regulating role in the mineralization of litter and soil organic matter (Gärdenäs et al., 2011; Melillo et al., 2011). The availability of N and P is likely to limit future carbon storage under climate change and rising atmospheric CO_2. Empirical stoichiometry observations were applied in the posteriori estimates of future carbon storage from land surface models (LSMs) lacking an explicit simulation of N and P biogeochemistry, which led consistently to an overestimation of future carbon storage in LSMs (Hungate et al., 2003; Wang and Houlton, 2009; Zaehle et al., 2015; Wieder et al., 2015). Nevertheless, this approach has large uncertainties (Penuelas et al., 2013; Sun et al., 2017) and relies on unproven assumptions (Brovkin and Goll, 2015).

An alternative is to represent directly the complex interactions between N, P and carbon in a LSM. Several LSMs incorporated different parameterizations of N interactions (e.g. Thornton et al., 2007; Zaehle et al., 2014) but very few global models have included P interactions. The few models accounted for P limitation in plant growth showed that P availability limit primary productivity and carbon stocks on highly weathered soils of the tropics (Wang et al., 2010; Yang et al., 2014) and one study also suggested that P limitations could also occur in the northern hemisphere in the near future (Goll et al., 2012). Model representations of P interactions are highly uncertain since the critical processes are poorly constrained by current observational data. In particular, the desorption of P from soil minerals surface and the enhancement of P availability for plants by phosphatase enzymes secreted by plant roots and microbes were identified to be critical but poorly constrained (Fleischer et al., 2019).

Previous studies (Wang et al., 2010; Goll et al., 2012; Yang et al., 2014; Thum et al., 2019) have suggested that the inclusion of the phosphorus cycle improves model performances with regard to reproducing observed C fluxes. But adding new and uncertain P-related processes does not grant an automatic improvement of a LSM in general. First, more (nutrient-related) equations with more uncertain parameters can result in less robust predictions. Second, models ignoring nutrients were often calibrated on available carbon data, so that a new model with nutrients inevitably needs a parameter recalibration to reach the similar performances as the same model without nutrients. Third, for evaluating a large-scale model resolving both nutrient and carbon biogeochemistry, one needs specific nutrient related datasets which are more scarce than classical biomass, productivity, soil carbon data used for benchmarking carbon only models.

The evaluation for N and P together with carbon cycling in global LSMs remains very limited (Wang et al., 2010; Goll et al., 2012) but recent advances in ground-based measurements, ecological datasets and process understanding have made a better evaluation of C, N, P models feasible. The available nutrient datasets have allowed for meta-analyses of site-level nutrient fertilization experiments (e.g. Yuan and

Chen, 2015; Wright, 2019), data-driven assimilation schemes to constrain nutrient budgets (Wang et al., 2018), new knowledge about the critical P-processes of sorption (Helfenstein et al., 2018; 2020) and phosphatase-mediated mineralization (Sun et al., 2020), global datasets of leaf nutrient content (Butler et al., 2017), and empirical constraints on the CO_2 fertilization effect on land carbon storage (Terrer et al., 2019; Liu et al., 2019). In addition to direct comparison with nutrient datasets, it is also possible to diagnose emerging model responses in terms of ecosystem resource use efficiencies (RUE) and confront them to observations for identifying how ecosystems adjust and optimize nutrient, water, light, and carbon resource availabilities (Fernández-Martínez et al., 2014; Hodapp et al., 2019). In particular, modeled N and P use efficiencies can be compared to observation-based estimates at ecosystem scale (Gill and Finzi, 2016) and at biome scale (Wang et al., 2018).

Here we evaluate the global cycles of C, N and P in the nutrient-enabled version of the LSM ORCHIDEE, ORCHIDEE-CNP (v1.2). The model has been previously evaluated for tropical sites (Goll et al., 2017a, 2018) and for coarse scale global carbon fluxes and stocks using the International Land Model Benchmarking system iLAMB by e.g. Friedlingstein et al., (2019). The results from this evaluation showed a slightly worse performance for ORCHIDEE-CNP (v.1.2) than the carbon-only version of ORCHIDEE which has been extensively calibrated (Friedlingstein et al., 2019). In this study, we perform a detailed evaluation of ORCHIDEE-CNP focusing on four ecosystem characteristics which were found to be critical for the response of land C cycling to increasing CO_2 and climate change: (1) vegetation resource use efficiencies, (2) the response of plant productivity to increasing CO_2, (3) ecosystem N and P turnover and openness, and (4) large-scale pattern of ecosystem stoichiometries. Point (1) and (2) control the response of vegetation carbon storage operating on timescales of years to decades, while point (3) and (4) control the carbon storage potential on ecosystem-level which determines the response on much longer timescales. Further, the implications of including nutrient cycles on the simulated land C cycling are discussed.

2 Modelling

2.1 Model description

ORCHIDEE-CNP simulates the exchange of greenhouse gases (i.e. carbon dioxide, nitrous oxide), water and energy at the land surface and features a detailed representation of the root uptake of dissolved N and P, the allocation of N and P among tissues, and the N and P turnover in litter and soil organic matter (Goll et al., 2017a, 2018) (Fig. 1). In this study, we present the first global application of the model and an evaluation against global carbon and nutrient datasets. ORCHIDEE-CNP simulates the cycles of C, N and P which are described in detail elsewhere (Krinner et al., 2005; Zaehle and Friend 2010; Goll et al., 2014, 2017a, 2018). We here give a brief overview. P enters the ecosystem by release from minerals into the soil solution, whereas N is biologically fixed from an ample reservoir of dinitrogen. Dissolved nutrients are either taken up by vegetation, converted into soil organic matter or absorbed onto soil particles. Losses occur as leaching of dissolved nutrients, gaseous soil N emissions, or occlusion of P in secondary minerals. When nutrients are taken up by vegetation they are either stored internally or used to build new plant tissue driven by the availability of C, N and P in vegetation.

The nutrient concentration of plant tissue varies within a prescribed range depending on the relative availability of C, N and P. Before plant tissue is shed, depending on the tissue a fixed fraction of the nutrients is recycled. The nutrients contained in dead plant tissue and organic matter are mineralized and released back into the soil solution. The model version applied in this study is based on Goll et al. (2017a, 2018) and referred to as ORCHIDEE-CNP v1.2. Major modifications compared to v1.1 are described as follows (details can be found in the Text S1).

The original formulation of photosynthetic capacity in ORCHIDEE-CNP v1.1 assumed leaf N to be the sole regulator of leaf photosynthetic characteristic (Kattge et al., 2009). Here, we applied a new empirical function that relates photosynthetic capacity to both leaf N and P concentration based on data from 451 species from 83 different plant families (Ellsworth et al., in prep.). A priori and narrow plant functional type (PFT)-specific range of leaf C:N:P ratios that were prescribed in ORCHIDEE-CNP v1.1 are now given a larger range common to all PFTs (Table S1), allowing for the prediction of variation of leaf stoichiometry across climate and soil gradients, independently of the prescribed vegetation (PFT) map.

In ORCHIDEE-CNP v1.1, an empirical function, $f(T_{soil})$ was used to reduce biochemical mineralization and plant nutrient uptake at low soil temperature (Eq.5 in Goll et al., 2017a) which was adopted from the N enabled version of ORCHIDEE (Zaehle and Friend, 2010) to avoid an unrealistic accumulation of N within plants when temperatures are low. We found that this function was not needed when P uptake is accounted for and was thus removed. It should be noted that this temperature dependence is different from the one which describes the temperature dependence of soil organic matter (SOM) and litter decomposition. For grasslands and croplands, we implemented root dormancy which is triggered by drought or low temperatures. During dormancy, root maintenance respiration is reduced by 90% following (Shane et al., 2009) but root acquisition of soil nutrients continues as long as root biomass exists (Malyshev and Henry, 2012). It should be noted that total root loss can occur for extremely long droughts or cold periods when maintenance respiration depletes root carbon.

Several parameters were re-calibrated, i.e. the coefficient relating maintenance respiration to biomass and the leaf to sapwood ratio, or corrected in case of the turnover of sapwood for tropical evergreen broadleaf forest (TREBF) and tropical rain-green broadleaf forest (TRDBF) to achieve more realistic wood growth rates for those forests (not shown). We also adjusted the recycling efficiency of nutrients from root ($f^N_{trans,root}$, $f^P_{trans,root}$) and leaf ($f^N_{trans,leaf}$, $f^P_{trans,leaf}$) according to data compilations from Freschet et al. (2010) and Vergutz et al. (2012). The new values of these parameters and their sources are given in Supplementary Information (Text S1).

2.2 Simulation setup

We performed a global simulation at 2^o x 2^o spatial resolution for the historical period (1700-2017) adapting the TRENDY version 6 protocol (Sitch et al., 2015; Le Quéré et al., 2018). The simulation was performed using historical climate forcing, land cover changes and management (i.e. mineral fertilizer application, crop harvest, see 3.1.6), and atmospheric CO_2 concentrations (S3 type simulation). Prior to the historical simulation, we performed a model spin-up to equilibrate the C, N and P pools and fluxes

(Sect. S1A in supplement) by forcing the model with cycled climate forcing of 1901-1920 and the land cover map and land management corresponding to the year 1700. To disentangle the effect of introducing nutrient cycles into ORCHIDEE, we performed the same simulation with ORCHIDEE (revision 5375) which has no nutrient cycles and a comparable parameterization for other processes. ORCHIDEE was run at a higher spatial resolution (0.5^{o}x0.5^{o}) than ORCHIDEE-CNP. Prior to the analysis, the data from ORCHIDEE was remapped to the resolution of ORCHIDEE-CNP.

2.2.1 Meteorological data

The model was forced by CRU-JRA-55 meteorological data provided at a spatial resolution of 0.5^{o} x 0.5^{o} and upscaled to a resolution of 2^{o} x 2^{o}. This data comprises global 6-hourly climate forcing data providing observation-based temperature, precipitation, and incoming surface radiation. It is derived from Climatic Research Unit (CRU) TS3.1 monthly data (Harris et al., 2014) and the Japanese 55-year Reanalysis (JRA-55) data (Kobayashi et al., 2015), covering the period 1901 to 2017. This climate dataset was provided by the TRENDY-v6 model-intercomparison project (Le Quéré et al., 2018).

2.2.2 Land cover

The historic land-cover change maps were based on the European Space Agency Climate Change Initiative (ESA-CCI) land-cover data (Bontemps et al., 2013). To be used by global vegetation models ORCHIDEE-CNP, ESA-CCI land-cover data were aggregated to $2^{o} \times 2^{o}$, and grouped into PFTs using the reclassification method from Poulter et al. (2011, 2015). The fraction of cropland and pasture in the PFT map was further constrained by the cropland area and the sum of pasture and rangeland area of the year 2010 in the History Database of the Global Environment land use data set (HYDE 3.2; Klein Goldewijk et al., 2017a, b) respectively, which were also aggregated to $2^{o} \times 2^{o}$. The above processes produced a reference ESA-CCI-based PFT map for the year 2010. The land-use changes derived from and Land-Use Harmonization (LUH) v2 (http://luh.umd.edu/data.shtml; an update release of Hurtt et al., 2011) were aggregated to $2^{o} \times 2^{o}$ and then were applied to this reference PFT map to constrain the land-cover changes of forest, grassland, pasture and rangeland, and cropland during the period 1700-2017 using the backward natural land cover reconstruction method of Peng et al. (2017). As a result, a set of historic PFT maps suitable for global vegetation models were established distinguishing global land-cover changes for the period of 1700-2017 at $2^{o} \times 2^{o}$ resolution.

2.2.3 Soil and lithology datasets

ORCHIDEE-CNP v1.2 is forced by information on soil texture, pH, bulk density and soil types (Goll et al., 2017a). We used a global gridded map of three soil texture classes from Zobler (1986) to derive soil-texture-specific parameters for soil water capacity, hydraulic conductivity and thermal conductivity. We used global gridded data on bulk density from the Harmonized World Soil Database (HWSD, 30 FAO/IIASA/ISRIC/ISSCAS/JRC, 2012) and soil pH from International Geosphere-Biosphere Programme Data Information System Soil Data (Global Soil Data Task Group, 2000). Soil pH forcing maps are needed to simulate the dynamics of NH_3 and NH_4^+ in soil in ORCHIDEE (Zaehle and Friend, 2010). We used a global gridded map with the dominant soil orders (following the USDA Soil

Taxonomy) at 1^{o}x1^{o} resolution to derive soil order specific soil phosphorus sorption parameters (Goll et al., 2017a).

The release of P from chemical weathering of rocks is computed dynamically following Goll et al. (2017a) and depends on the lithology types and soil shielding (discontinuation of the active soil zone from the bedrock) (Hartmann et al., 2014). We used the global lithological map (GLiM) of Hartmann and Moosdorf (2012) upscaled to 1^{o} x 1^{o} resolution which accounts for the lithology fractional coverage of 16 classes on a sub-grid scale. We also used a spatial explicit map of soil shielding on a 1^{o} x 1^{o} resolution (Hartmann et al., 2014).

2.2.4 Atmospheric nitrogen and phosphorus deposition

Global gridded monthly atmospheric N and P deposition during 1860-2017 was derived from a reconstruction based on the global aerosol chemistry–climate model LMDZ-INCA (Wang et al., 2017). LMDZ-INCA was driven by emission data, which included sea salt and dust for P, primary biogenic aerosol particles for P, oceanic emissions for N (NH_3), vegetation emissions for N (NO), agricultural activities (including fertilizer use and livestock) for N and fuel combustion for both N (NO_y and NH_x) and P. Reconstructions for the years 1850, 1960, 1970, 1980, 1990, and each year from 1997 to 2013 were linearly interpolated to derive a time series for 1850-2013. For the period before 1850, we assumed N and P deposition rates of the year 1850. For the period after 2013, we assumed rates of the year 2013. In ORCHIDEE-CNP, atmospheric N and P deposition are added to the respective soil mineral N and P pools without considering interception by the canopy.

2.2.5 Nutrient management

For croplands, we used yearly gridded mineral N and P fertilizer application data from Lu and Tian (2017) available for the period 1960 to 2017. This dataset is based on national-level data of crop-specific fertilizer application amounts from the International Fertilizer Industry Association (IFA) and the FAO. N and P mineral fertilization between 1900 and 1959 were linearly extrapolated assuming that fertilizer applications for 1900 are zero, and that there were no N and P fertilizers applied before 1900. For pasture, we used global gridded datasets of mineral N fertilizer application rates from Lu and Tian (2017), developed by combining country-level statistics (FAO) and land use datasets (HYDE 3.2) (Xu et al., 2019). For both cropland and pasture, N and P in mineral fertilizer was assumed to go directly into soil mineral pools, where all mineral N fertilizer was assumed to be in the form of ammonium nitrate, that is half of N as ammonium (NH_4^+) and half as nitrate (NO_3^-).

Manure applications are also included as a model forcing, given their significant input contribution to agricultural soils. For cropland, we used gridded annual manure N application data for the period 1860–2014 from Zhang et al. (2017) compiled and downscaled based on country-specific annual livestock population data from FAOSTAT. For the period before 1860, we assumed N and P deposition rates of the year 1860. For pasture, we used global gridded datasets of N manure application rates from Lu and Tian (2017). The application of manure P in cropland and pasture was derived from manure N assuming a manure P:N ratio of 0.2. This ratio is a weighted value by the amount of manure N applied to soil and

derived from ruminants (14.4 Tg N yr^{-1}) and monogastric animals (10.1 Tg N yr^{-1}) from FAOSTAT for the year 2000 with P:N ratios of 0.165 in ruminant manure (mean of 0.15-0.18 from Lun et al., 2018) and 0.26 in monogastric manure (mean of 0.24-0.28 from Lun et al. (2018)). For manure applied to cropland and pasture, we assumed a typical slurry application with 90% of N in the liquid part of the slurry (like urine) goes to soil $NH4^+$ pool. For the solid part of the slurry, we assumed it goes to a litter pool with a C:N ratio of 10:1 following Soussana and Lemaire (2014).

Mineral and manure N and P fertilizers in cropland were applied at day of year (DOY) 120 for northern hemisphere (30°N - 90°N), at DOY 180 for tropical regions (30°N - 30°S), and at DOY 240 for southern hemisphere (30°S - 90°S).

3 Evaluation

We evaluated the performances of ORCHIDEE-CNP v1.2 based on four major aspects (Fig. 1). Firstly, we evaluated the global C, N and P flows and storages. In the absence of robust spatially resolved estimates of N and P fluxes, we used the data-driven reconstruction of steady state C, N and P fluxes on biome level from the data assimilation system Global Observation-based Land-ecosystems Utilization Model of Carbon, Nitrogen and Phosphorus (GOLUM-CNP) v1.0 (Wang et al., 2018) (Table 1). Secondly, we evaluated plant resource use efficiencies (RUE) of light, water, C, N and P on global and biome scales. RUEs reflect how ecosystems adjust and adapt to the availability nutrient, water, light, and carbon resources (Fernández-Martínez et al., 2014; Hodapp et al., 2019). For this, we used estimates from site measurements and observation-based gridded datasets. Thirdly, we evaluated the response of GPP to elevated CO_2 to assess the response of plant productivity to changing resource availability (i.e. CO_2) historical perturbation C fluxes. For this, we used observation-based estimates (Ehlers et al., 2015; Campbell et al., 2017). Fourthly, we evaluated large scale patterns of vegetation and soil N:P ratios as well as the N and P openness and turnover rates on ecosystem-level to assess spatial variation in nutrient limitation and the underlying drivers. For this, we used estimates from GOLUM-CNP, site measurements and observation-based gridded datasets (Kerkhoff et al., 2005; McGroddy et al., 2004; Reich and Oleksyn, 2004; Tipping et al., 2016; Butler et al., 2017; Wang et al., 2018). Finally, we showed the implications of ORCHIDEE-CNP for C cycling by evaluating the spatiotemporal patterns of terrestrial C fluxes and pools of the two versions of ORCHIDEE. For this, we used observation-based products of GPP and atmospheric inversions of the net land-atmosphere CO_2 flux excluding fossil fuel emissions (Table 1). Each dataset is summarized in Table 1 and described in detail in the Supplementary Information. All the gridded datasets with high spatial resolutions (Table 1) were resampled to the 2° x 2° resolution of the model output using area-weighted mean methods.

3.1 Ecosystem productivity

Different data-driven maps of NPP and GPP based on remote sensing and climate datasets were used (Table 1), thereby accounting for the uncertainty of each product as well as for the uncertainty from the spread between different products. Uncertainties of each NPP and GPP product were derived according to original publications. We used a 20% uncertainty of gridded GPP from Moderate Resolution Imaging

Spectroradiometer (MODIS) and Breathing Earth System Simulator (BESS) (Sect. S1C in the supplement; Turner et al., 2006; Jiang and Ryu, 2016) at 2° scale. This is a coarse extrapolation of uncertainty reported at grid-cell scale, since none of these products reported spatial error covariance information allowing to up-scale this uncertainty at 2° resolution. Further, for some products, uncertainty was defined as the bias against local measurements (Turner et al., 2006) and for others by using different climate input fields (Table 1). For Multi-Tree-Ensemble (MTE)-GPP (Table 1), we used the spread (1-sigma standard deviation) from an ensemble of 25 members produced by different machine learning methods (Jung et al., 2009). For MODIS-NPP (Table 1), we used a 19% uncertainty as assessed by Turner et al. (2006). For BETHY-NPP we do not have an uncertainty (Tum et al., 2016). For Global Inventory Modeling and Mapping Studies (GIMMS)-NPP (Table 1), we used the variance of three sets of products (Table 1) based on different climate datasets (Smith et al., 2016).

Two statistical indices were used to summarize the performance of ORCHIDEE and ORCHIDEE-CNP with respect to inter-annual and seasonal variability of GPP and inter-annual variability of Net biome productivity (NBP) (Sect. 4.6): coefficient of determination (R^2) and relative mean-square deviation (*rMSE*). *rMSE* is defined as:

$$rMSE = \frac{\sum_{j=1}^{n}(X_{model,j} - X_{ref,j})^2}{\sum_{j=1}^{n}(X_{ref,j} - \hat{X}_{ref,j})^2} \quad (1)$$

X_{model} and X_{ref} are values from models (i.e. ORCHIDEE and ORCHIDEE-CNP) and referenced datasets (i.e. MTE and BESS, Sect. S1C in supplement) respectively, $\hat{X}_{ref,j}$ is the mean value across all years (for inter-annual variability evaluation) or all months (for seasonality evaluation).

3.2 Resource use efficiencies

The definition of resource use efficiencies is explained in Sect. 4.2. Observation-based light use efficiency (LUE) was calculated using MTE-GPP, downward shortwave radiation from CRUJRA, and fraction of Absorbed Photosynthetically Active Radiation (fAPAR) from the Global SeaWiFS Level-3 data (Gobron et al., 2006a, b). Uncertainty was derived from 25 ensemble members of MTE-GPP. Observation-based water use efficiency (WUE) was calculated as the ratio between MTE-GPP and MTE-ET (Table 1); its uncertainties were calculated using a Monte-Carlo resampling procedure in which 25 different members of GPP and ET were randomly selected. Observation-based carbon use efficiency (CUE) was calculated from the ratio of MODIS-NPP to MODIS-GPP. It should be noted that MODIS-NPP is based on a calibrated version of the BIOME-BGC model (Turner et al., 2006) so that CUE is not strictly an observation-based quantity. CUE uncertainties were calculated using a Monte-Carlo method given a 20% and 19% uncertainty for MODIS GPP and NPP products at 2° resolution, respectively.

4. Results

4.1 Carbon, nitrogen and phosphorus flows and storages

We compared the simulated fluxes of C, N and P within natural ecosystems for the period 2001-2010 to the data-driven estimates from GOLUM-CNP (Table 1; Sect. S1B in supplement) on the global scale and for natural ecosystems at biome-scale. Modelled global C, N and P fluxes in ORCHIDEE-CNP are comparable with the estimates by GOLUM-CNP (Fig. 2). One exception is that ORCHIDEE-CNP simulates a four-fold lower P leaching from soils (3.7 ± 9.7 mg P $m^{-2}yr^{-1}$) than GOLUM-CNP (23 mg P $m^{-2}yr^{-1}$) (Fig. 2), which mainly occurs in forest ecosystems (Fig. S1). Note that GOLUM-CNP presents the steady-state C, N and P cycles in natural biomes, omitting human perturbations which have strongly altered the flows of C, N and P during the recent past. The impact of such perturbations on the nutrient flows are analyzed in detail in Sect. S2 and S3 in supplement.

In terms of C and nutrient storages, ORCHIDEE-CNP simulated comparable soil C, N and P storage (soil organic matter and litter) but higher vegetation C, N and P than GOLUM-CNP. Detailed comparisons for spatial pattern of SOC and forest above ground C against observation-based datasets can be found in Figs. S2 and S3.

4.2 Resource use efficiencies

We evaluate here the resource use efficiencies of GPP for light (L), water (W), C, N and P defined by:

$$LUE = \frac{GPP}{fAPAR \times PAR}, \quad (2)$$

$$WUE = \frac{GPP}{ET}, \quad (3)$$

$$CUE = \frac{NPP}{GPP}, \quad (4)$$

$$NUE = \frac{GPP}{F_N}, \quad (5)$$

$$PUE = \frac{GPP}{F_P}, \quad (6)$$

Where GPP is the annual gross primary productivity (g C m^{-2} yr^{-1}), fAPAR the fraction of absorbed photosynthetically active radiation (%), PAR is annual Photosynthetically Active Radiation (W m^{-2} yr^{-1}), ET the annual evapotranspiration (mm m^{-2} yr^{-1}), F_N and F_P the total N uptake (g N m^{-2} yr^{-1}) and P uptake by plants (g P m^{-2} yr^{-1}), respectively. We calculated fAPAR in ORCHIDEE-CNP and ORCHIDEE as a function of leaf area index (LAI): fAPAR=1-exp(-0.5 · LAI) (Ito et al., 2004).

Compared to observed LUE (Sect. S1E in supplement), ORCHIDEE-CNP modelled median values at biome level are generally lower, but still within the ranges of uncertainties of observation-based datasets (Sect. 3.2) excepted for tropical (TRF) and temperate deciduous forests (TEDF). In comparison to

ORCHIDEE, ORCHIDEE-CNP simulated LUE which are closer to observation for 4 out of 6 biomes (TECF, BOCF, TEG, TRG) (Fig. 3a).

Compared to observed WUE, ORCHIDEE and ORCHIDEE-CNP simulated values fall within the uncertainty range of observations (Fig. 3b). However, the WUE values from ORCHIDEE-CNP are on the high end of the range for temperate conifers (TECF) and BOCF and on the low end for temperate and tropical grasslands (TEG and TRG). The highest median WUE were correctly simulated in temperate forests by ORCHIDEE-CNP (Fig. 3b), but the lowest WUE values were simulated in temperate instead of tropical forests.

Compared with observed CUE, ORCHIDEE-CNP simulated comparable values for TEDF and TECF but lower values for TRF, BOCF and grasslands. Both ORCHIDEE-CNP and ORCHIDEE cannot capture the increase of CUE from tropical to boreal forests apparent in the observation-based products (Fig. 3c) and in measurements from forest sites (Piao et al., 2010). In comparison to ORCHIDEE, ORCHIDEE-CNP simulated CUE which are closer to observation for 4 out of 6 biomes (TEDF, TECF, BOCF, TEG) with respect to median and spread.

Consistent with site-observations of NUE from Gill and Finzi (2016) and GOLUM-CNP outputs, ORCHIDEE-CNP simulated correctly the high values of TECF and the low values of tropical forests (Fig. 4a). However, compared with site-observations of PUE from Gill and Finzi (2016) showing a PUE decrease from tropical to boreal region, ORCHIDEE-CNP simulated a rather flat value (Fig. 4b). This suggests a too strong P limitation in high latitude ecosystems, consistent with the fact that the model underestimates peak northern GPP and the northern land sink (Sect. 4.6). Nevertheless, the model simulated PUE values falls in the range of GOLUM-CNP estimates. Tropical C4 grasslands have higher simulated NUE and PUE than temperate C3 grasslands, consistent with GOLUM-CNP (Fig. 4).

4.3 CO_2 fertilization effect

We compare the simulated response of plant productivity to increasing CO_2 during the historical period (i.e., CO_2 fertilization effect Eco_2) to observation-based estimates for C3 plants from historical change of deuterium isotopomers in leaf herbarium samples (Ehlers et al., 2015) and for global (C3 and C4) vegetation to indirect evidence from carbonyl sulfide (COS) atmospheric ice-core observations (Campbell et al., 2017). The CO_2 fertilization effect is here defined by the GPP ratio (Eco_2):

$$E_{co2} = \frac{GPP_{396}}{GPP_{296}}, \quad (7)$$

where GPP_{296} indicates pre-industrial GPP (g C m^{-2} yr^{-1}) under CO_2 concentration of 296 ppm and GPP_{396} under current CO_2 concentration of 396 ppm. Those CO_2 concentrations of 296 ppm and 396ppm correspond to tropospheric mixing ratio of CO_2 in year ~1900 and 2013 respectively, similar to values used for estimating the response of GPP to a ~100 ppm CO_2 increase in Ehlers et al. (2015) and Campbell et al. (2017).

Modeled Eco_2 by ORCHIDEE-CNP of natural biomes ranges between 1.0 and 1.3 for most regions (Fig. 5a), slightly lower than global Eco_2 derived from COS of 1.26-1.36 (Campbell et al., 2017). Modeled Eco_2 for C3 plants (Fig. 5c, Fig. S4) are also consistent with Eco_2 from herbarium samples (Ehlers et al., 2015) equal to 1.23. When compared to ORCHIDEE without nutrient cycles, we found that ORCHIDEE-CNP simulates smaller and more realistic values of Eco_2 (Fig. 5c, d), yet with lower values in boreal regions that could not be checked against observations (Fig. S5).

4.4 Ecosystem nutrient openness and nutrient turnover

Nutrients taken up by plants are either recycled within the ecosystem or acquired from external sources (P weathering of primary and secondary minerals, atmospheric N and P deposition, biological nitrogen fixation (BNF), and N and P fertilizer addition to cultivated lands). Wang et al. (2018) calculated an indicator of the openness of N and P cycling in natural ecosystems as the ratio of external inputs of N and P into the ecosystem to the total amount of N and P that plants use for GPP. Similarly, we diagnosed the openness for N and P (O_N and O_P) from the ORCHIDEE-CNP output by:

$$O_x = \frac{I_x}{F_x + RSB_x}, \quad (8)$$

where I_x is the annual external nutrient input (gX m^{-2} yr^{-1}), F_x the annual plant uptake of soil nutrients (gX m^{-2} yr^{-1}), and RSB_x the flux of nutrients recycled within plants (gX m^{-2} yr^{-1}) by foliar nutrient resorption prior to leaf shedding. External nutrient inputs include atmospheric N deposition and BNF, and include P deposition and P release from rock weathering.

Modelled O_N in natural biomes by ORCHIDEE-CNP showed only a small variance across the globe, whereas GOLUM-CNP predicts a higher O_N in tropical and temperate regions than in boreal regions (Fig. 6a, b). O_P values are below 15% in ORCHIDEE-CNP for most biomes, of similar order of magnitude than in GOLUM-CNP (Fig. 6c, d). ORCHIDEE-CNP simulates a lower O_N in tropical natural biomes than GOLUM-CNP, which is mainly due to lower but more realistic tropical BNF in ORCHIDEE-CNP compared to GOLUM-CNP (Sect. S4 in supplement). ORCHIDEE-CNP simulates a higher O_N in high latitudes grassland (Fig. 6a, b) than GOLUM-CNP, which is due to overestimation of BNF in NH in ORCHIDEE-CNP (Sect. S4 in supplement). Modelled O_P in natural biomes by ORCHIDEE-CNP compares well with GOLUM-CNP except for central Africa (Fig. 6c, d). This is primarily because ORCHIDEE-CNP used a lower P deposition forcing than GOLUM-CNP.

Residence time quantifies the average time it takes for a N (or P) molecule from entering to leaving the ecosystem (τ_N and τ_P). In this study, we adopted the approach of Carvalhais et al. (2014) for the carbon residence time. We define the residence time of N and P as the ratio of total respective nutrient stock in the ecosystem to their respective total input flux:

$$\tau_N = \frac{\sum_{i=1}^{5} N_i + N_{inorg}}{N_d + BNF}, \quad (9)$$

$$\tau_P = \frac{\sum_{i=1}^{5} P_i + P_{inorg}}{P_d + P_w}, \quad (10)$$

where N_i indicates the N mass (g N m^{-2}) in organic matter pools i (with i = plant, litter, SOM pools); N_{inorg} is the sum of all inorganic N pools, N_d and BNF are N deposition and biological N fixation rates respectively (g N m^{-2} yr^{-1}). Similarly, P_i is the P mass (g P m^{-2}) in organic matter pools, P_{inorg} the sum of inorganic P pools, and P_d and P_w are P deposition and P weathering release rates, respectively (g P m^{-2} yr^{-1}).

Modeled median τ_N of natural biomes in ORCHIDEE-CNP varies between 56-1585 years, while τ_P varies within a large range of 101 to 223870 years (Fig. 7). ORCHIDEE-CNP captured the order of magnitude of τ_N and τ_P for forests found in GOLUM-CNP. Longer median τ_N (1585 years) and τ_P (1223870 years) are simulated for boreal forest compared to temperate and tropical forests (251-794 years for τ_N and 891-7080 years for τ_P) and grassland (56-158 years for τ_N and 101-468 years for τ_P) by ORCHIDEE-CNP, consistent with results from GOLUM-CNP. However, for grasslands, simulated τ_N (56-158 years) and τ_P (101-468 years) are 5-11 folds shorter than in GOLUM-CNP (Fig. 7).

4.5 Stoichiometry

4.5.1 Foliar stoichiometry

Leaf N:P ratios for natural biomes predicted by ORCHIDEE-CNP vary between 15~25 (Fig. 8a). The observed decline in median leaf N:P ratios with increasing latitude was not reproduced by the model (Sect. S1E1 in supplement; Fig. 8e), although the modelled latitudinal distribution of leaf N:P ratios remained within the 10~90th quantiles of the site level data (Kerkhoff et al., 2005; McGroddy et al., 2004; Reich and Oleksyn, 2004). Further, the simulated leaf N:P ratios fall within the interquartile of upscaled site measurements by Butler et al. (2017) for most of the globe, with the exception of regions north of 55°N where leaf N:P are outside the observation-based range, suggesting a too strong P constraint relative to N (Fig. 8).

4.5.2 Soil stoichiometry

We evaluate here the modelled C:N, C:P and N:P ratios of soil organic matter for different biomes against data from the large compilation of measurements for soils (0-60cm depth) by Tipping et al. (2016). Modelled C:N ratios fall into much more narrow ranges (7.8~11.8 for the widest interquartile range) compared to the observations (11.1~20.5; Fig. 9a), as a result of prescribing constant C:N ratios in ORCHIDEE-CNP (Goll et al., 2017a). SOM P content varies in ORCHIDEE-CNP as a consequence of varying biochemical phosphorus mineralization rates (Sect S7 in supplement) and thus C:P and N:P ratios of SOM show pronounced variation in space. ORCHIDEE-CNP simulates comparable N:P ratios than measurements in terms of both median value and distributions for tropical forests, but overestimates the observed N:P ratios by 108-327% in temperate forests, tropical and temperate grasslands soils (Fig. 9b, c). The higher observed C:P and N:P in forest compared to grassland soils are not captured by ORCHIDEE-CNP (Fig. 9b, c). We also compared ORCHIDEE-CNP N:P ratios to the results of GOLUM-CNP which were based on the data from Zechmeister-Boltenstern et al. (2015),

more limited than Tipping et al. (2016) and found an overestimation for temperate forests, tropical and temperate grasslands.

4.6 Nutrient effects on carbon cycling

We analyze the performance of ORCHIDEE-CNP v1.2 and ORCHIDEE without nutrient cycles with respect to the spatiotemporal patterns of GPP, NPP and net biome productivity.

Global GPP and NPP simulated by ORCHIDEE-CNP averaged over the period 2001-2010 are 119 PgC yr^{-1} and 48 PgC yr^{-1} respectively, both within ranges of the data-driven products listed in Table 1 (Sect. S1C in supplement; Table S2). GPP and NPP simulated by ORCHIDEE-CNP are lower than those simulated by ORCHIDEE (140 Pg C yr^{-1} for GPP and 60 Pg C yr^{-1} for NPP). The values from ORCHIDEE are on the high end of the range of estimates from the data-driven products of Table 1. ORCHIDEE-CNP simulated comparable GPP values for most parts of the globe (Fig. S6a), and comparable NPP values for most of northern high-latitudes (Fig. S6b), which lie within the range given by the data-driven products.

Inter-annual and seasonal variations of GPP reflect the response of ecosystems to inter-annual or seasonal climatic variability, as well as the effects of natural (e.g. fires, wind throw, insect outbreaks, and storms) and anthropogenic disturbances (e.g. land management and land cover change) (Anav et al., 2015). Regarding the inter-annual anomalies of de-trended GPP (GPP_{int}) for the period 2001-2011, estimations on global scale from ORCHIDEE-CNP show rather good correlation with observation-driven model BESS-GPP (R^2 =0.71), but not with MTE-GPP (R^2 =0.11) (Fig. 10a). ORCHIDEE performs somewhat worse on global scale than ORCHIDEE-CNP, primarily due to its low performance in the NH. We find that inclusion of nutrients in ORCHIDEE leads to a lower model predictions error on global scale and for all latitudinal bands irrespectively of the observation-based product (Fig. 10a).

Regarding the seasonal variation of GPP over the period 2001-2011, the predictions of ORCHIDEE-CNP are in good agreement with observation based estimates and show no significant differences when compared to ORCHIDEE, except for tropical regions (Fig. 10b). Here, the model errors in seasonal variations of GPP are substantially larger for ORCHIDEE-CNP than for ORCHIDEE (Fig .10b).

Net biome productivity (NBP) is defined as the net C exchange between the atmosphere and the terrestrial biosphere, that is the sum of net primary productivity, heterotrophic respiration and emissions due to disturbances; positive values denoting a land carbon sink. Compared to the three sets of atmospheric inversions (CAMS, JENA and CTracker), ORCHIDEE(-CNP) performs slightly worse than the mean of predictions from 16 land surface models from Trendy ensembles (v6) (Fig. 10c). ORCHIDEE-CNP shows a worse performance in inter-annual variability of NBP than ORCHIDEE when compared against inversion datasets at global scale and for the Northern Hemisphere. However, ORCHIDEE-CNP improved the performance of inter-annual variability of NBP against inversion datasets relative to ORCHIDEE for tropical region (higher R^2 and lower rMSE) with closer or even better fitness against inversion datasets than the mean value of Trendy ensemble models (Fig. 10c).

5. Discussion

We performed a detailed evaluation of ORCHIDEE-CNP in terms of four nutrient-related ecosystem properties which control ecosystem gas exchanges and carbon storage: vegetation resource use efficiencies, CO_2 fertilization effect, ecosystem N and P turnover and openness, and large-scale pattern of ecosystem stoichiometries.

We find that the inclusion of nutrients tends to lead to improvements in simulated resource use efficiency of plant resources (light, carbon, water) on biome scale (Sect. 5.1). In line with changes in resource use efficiency, the sensitivity of GPP to variations in climate is improved leading to improved inter-annual variation in GPP, in particular for the Northern Hemisphere (Sect. 5.5). In addition, the response of GPP to increasing atmospheric CO_2 concentration is improved (Sect. 5.2). However, model biases in C fluxes remained or increased, for example in the NBP of the Northern Hemisphere. The analysis of nutrient use efficiencies (Sect. 5.1), stoichiometry (Sect. 5.4), as well as ecosystem openness and turnover of nutrients (Sect. 5.3) reveal biases in boreal regions which might be related to issues with too strong soil organic matter accumulation and the dependency of photosynthesis on leaf nutrients in needle-leaf PFTs. On a seasonal scale, we found a general deterioration of the simulated seasonal cycle of GPP due to the inclusion of nutrient cycles (Sect. 5.5).

In the following, we discuss in more detail the model performance with respect to nutrient cycles and their effects on simulated C fluxes, and propose ways to address model biases.

5.1 Inclusion of nutrient cycling improves use efficiencies of other plant resources

Resource use efficiency (RUE) is an ecological concept that measures the proportion of supplied resources, which support plant productivity, i.e. it relates realized to potential productivity (Hadapp et al., 2019). It is therefore a critical ecosystem property which relates resource availability to ecosystem productivity, as well as being affected by resource availability.

With the inclusion of additional plant resources nitrogen and phosphorus, changes in the simulated vegetation use efficiencies of resources like water (WUE), light (LUE) and carbon (CUE) are expected. Indeed, the annual use efficiencies on biome-scale differ between ORCHIDEE-CNP and ORCHIDEE. In comparison to observation-based estimates, the inclusion of nutrient cycles tends to improve simulated LUE and CUE and WUE (Fig. 3).

Both ORCHIDEE-CNP and ORCHIDEE generally underestimate annual LUE for forest biomes (Fig. 3a) which is due to a high bias in fAPAR in both models (28%-380% for ORCHIDEE, and 80%-173% for ORCHIDEE-CNP) (Fig. S4a, b). Although the bias in LUE for TRF is higher, the bias in GPP is largely reduced whereas the bias in fAPAR is similar in ORCHIDEE-CNP compared to ORCHIDEE (Fig. S4a, b), indicating general issues in ORCHIDEE with respect to how light is transferred within canopy in tropical forest. Both versions assume constant canopy light extinction coefficient of 0.5, omitting variations among biomes due their distinctive canopy architectures (Ito et al., 2004). Improving this part of the model requires a canopy light transfer scheme that better accounts of canopy

structure (Naudt et al., 2015) and the inclusion of different light components including diffuse incoming, scattered and direct light (Zhang et al. 2020).

ORCHIDEE-CNP simulated a lower WUE than ORCHIDEE with the exception of coniferous biomes (Fig. 3b). The improvement of WUE in TRF is related to improvements in GPP and ET, while the overestimation of WUE in coniferous dominated biomes by ORCHIDEE-CNP is related to an overestimation of GPP (Fig. S4 c). The latter is likely a result of the application of a relationship between photosynthetic capacity and leaf nutrient concentration which is based on measurements from broadleaf species for all PFTs. Kattge et al. (2009) showed that coniferous PFTs have a ~40% lower carboxylation capacity for a given leaf nitrogen concentration than other PFTs. The omission of this could explain the bias in coniferous GPP in ORCHIDEE-CNP. Uncertainties in evaluation datasets hamper a more detailed evaluation of the variations of WUE among biome types.

We found that the inclusion of nutrient cycles improved the spatial variability in simulated CUE, but general biases remain (Fig. 3c), and uncertainties in observation-based estimates are large. Improvements are mainly found in temperate biomes (TEDF, TECF and TEG), indicating the allocation of GPP to respiration and biomass growth, which is controlled by nutrient availability, works reasonably well. ORCHIDEE-CNP underestimates CUE for tropical biomes (TRF and TRG) more strongly than ORCHIDEE, despite substantially reduced biases in NPP and GPP (Fig. S4 d). However, we should be cautious in drawing conclusions considering the large uncertainty in MODIS CUE (He et al., 2018).

NUE, PUE on biome scale compare well to estimates (Fig. 4), indicating that ORCHIDEE-CNP is able to simulate the coupling strength between C, N and P cycles. However, ORCHIDEE-CNP underestimates PUE in tropical forests. A sensitivity analysis by GOLUM-CNP indicated that NUE and PUE were most sensitive to the NPP-allocation fractions (especially to woody biomass) and foliar stoichiometry (Wang et al., 2018). Therefore, we attribute the biases in PUE to the biases in foliar stoichiometry (Fig. 8) and to issues in plant internal P allocation in ORCHIDEE-CNP (Fig. S1).

5.2 Inclusion of nutrient cycling improves CO_2 fertilization effect

The effect of CO_2 fertilization on terrestrial ecosystem productivity is thought to be the dominant driver behind the current land carbon sink. The strength of the fertilization effect on GPP differs strongly between LSMs (Friedlingstein et al., 2014). We used proxies of the historical increase in GPP for an indirect model evaluation of the CO_2 fertilization effect from COS and deuterium measurements of herbarium samples (Ehlers et al., 2015; Campbell et al., 2017), and found that ORCHIDEE-CNP has smaller and more realistic Eco_2 than the same model without nutrients (Fig. 5), in particular for C3 plants and in boreal regions (Fig. S5). Both ORCHIDEE-CNP and ORCHIDEE simulated a Eco_2 for C4 grass of ~1, as the carboxylation of C4 plants is weakly influenced by elevated CO_2 (Osmond et al., 1982; Pearcy and Ehleringer, 1984; Bowes, 1993). This indicates that the inclusion of N and P constraints on GPP leads to a more realistic CO_2 fertilization effect in ORCHIDEE-CNP.

5.3 Ecosystem nutrient turnover and openness indicates model biases in boreal phosphorus availability

The capacity of ecosystems to sequester and store additional carbon depends on their ability to supply nutrients for the built-up of organic matter. Enhanced internal nutrient recycling or the accumulation of nutrients over time in ecosystems are theoretically possible mechanisms by which nutrients can be supplied. Therefore, it is important for simulating changes in land carbon storage on decadal time scales and longer that models capture the dependency of ecosystem production to external nutrient sources (i.e. openness of N and P cycles) (Cleveland et al., 2013) as well as the residence time of nutrients within ecosystems. Besides being related to each other, openness and residence times are also related with the in- and outflows of- nutrients (Eq. 9 and Eq. 10) as well as turnover time of nutrients in specific ecosystem compartments.

We find that ORCHIDEE-CNP simulates openness of nutrient cycles incl. differences among biomes which are close to estimates from the model–data fusion framework GOLUM-CNP (Fig. 6; Sect. 4.4). There are differences in openness of N (O_N) in tropical natural biomes and openness of P (O_P) in central Africa which are related to lower, but more realistic, tropical BNF in ORCHIDEE-CNP (Sect. S4 in supplement) and a difference in the prescribed P deposition compared to GOLUM-CNP. Simulated nutrient losses due to aquatic transport are in general in good agreement with independent estimates (Sect. S5 in supplement).

Residence times of N and P (τ_N and τ_P) in ORCHIDEE-CNP compare in general well to estimates from GOLUM-CNP: ORCHIDEE-CNP simulates shorter τ_N and τ_P in tropical and temperate biomes compared to boreal ones, in line with GOLUM-CNP (Fig. 7). This indicates that ORCHIDEE-CNP is able to reproduce large-scale patterns in the nutrient residence time of biomes, with one exception. In boreal regions, we find that ORCHIDEE-CNP simulates higher τ_P for BOCF due to the higher standing P stocks of biomass and soil organic matter than GOLUM-CNP (Fig. S1). This indicates that ORCHIDEE-CNP is likely underestimating P availability in boreal regions. The underlying processes of biochemical P mineralization (Sect. S7 in supplement) and sorption of P to soil particles (Sect. S6 in supplement) are reasonably well captured in ORCHIDEE-CNP.

5.4 Model biases in stoichiometry indicate need for refinement of process representation

Leaf and soil stoichiometry are key indexes to characterize the ecosystem relative N and P limitation (e.g. Güsewell, 2004). Measurements show a decrease in foliar N:P ratios from low to high latitudes in natural ecosystems (McGroddy et al., 2004; Reich and Oleksyn, 2004; Kerkhoff et al., 2005). This is seen as evidence for tropical vegetation being in general more P- than N-limited, in contrast to extra-tropical vegetation (Reich and Oleksyn, 2004). The observed trend of foliar N:P ratios was not reproduced by ORCHIDEE-CNP (Fig. 8) which simulated a flat foliar N:P latitudinal profile. In contrast to the majority of global models, where leaf N:P ratios are either prescribed (Goll et al., 2012) or vary within a PFT-specific range (Wang et al., 2010), we assumed conservatively a globally uniform range to let the model freely calculate leaf N:P stoichiometry. It is not trivial to pin down the failure of the model to capture the latitudinal trend in leaf N:P ratios, which could be due to: 1) omitted variability in leaf P resorption efficiencies, which varies among biomes between 46%~66.6% (Reed et al., 2012),

but was set to 65% in ORCHIDEE-CNP, 2) the simplistic parameterization of nutrient investment into different plant tissues, 3) and the omission of the diversity of nutrient acquisition pathways (e.g. mycorrhizal association) and rooting strategies (Warren et al., 2015). Testing new formulation for plant growth based on optimality principles (Kvakić et al., 2020) and the refinement of nutrient acquisition pathways (Sulman et al., 2017) are ways forward to improve the model.

Regarding soil stoichiometry, measurements show that tropical biomes have lower soil C:N and higher soil C:P and soil N:P than temperate biomes (Tipping et al., 2016), echoing the pattern of leaf stoichiometry. ORCHIDEE-CNP fails in capturing these patterns (Fig. 9). Modelled soil N:P and C:P for tropical forests are comparable to measurements but are too low in temperate forest, tropical and temperate grass, which is most likely related to a too strong nutrient immobilization in accumulating soil organic matter (Figs. S1) which tends to push systems into P limitation rather than N limitation as O_N is larger than O_P (Fig. 6). In general, the spread in soil P concentration is well represented by ORCHIDEE-CNP. The rudimentary representation of organic matter decomposition and the lack of nutrient effects on decomposers carbon use efficiency (see Zhang et al., 2018 for possible improvements, Sect. 5.5) are likely contributing to the biases. New developments including explicit representation of decomposer communities and soil organic matter stabilization (Zhang et al., 2020) will be included in the next model version.

5.5 Nutrient effects on carbon cycling

In the following we discuss the implications for the simulated carbon fluxes of changes in plant resource use efficiencies and the sensitivity of plant productivity to increasing CO_2 due the inclusion of nutrient cycles. We link biases in the simulated carbon fluxes to biases in nutrient cycling, which allows us to prioritize follow up model development.

5.5.1 Inclusion of nutrient cycling improves the inter-annual variability of GPP

To what extent nutrient effects on vegetation affect the sensitivity of ecosystem CO_2 fluxes to climatic variation is unclear (Goll et al., 2018). For instance, drought can reduce nutrient use by decreasing GPP, but it also slows down decomposition which supplies nutrients for plant uptake. Further, N:P stoichiometry is also strongly modified by drought and warming towards increased N:P in whole plant biomass (Yuan and Chen, 2015). Here we found that the inclusion of N and P cycles in ORCHIDEE affects the inter-annual variability of GPP for all vegetation types. In ORCHIDEE-CNP, the inter-annual variation (IAV) of GPP is better correlated to that of observation-based datasets than in ORCHIDEE globally and for the NH, but less correlated for other regions (Fig. 10a). Observation-based GPP estimates are uncertain, as some of them ignore soil moisture induced reductions of GPP during drought (Stocker et al., 2019), and soil thaw and snow-related effects (Jiang and Ryu, 2016). Thus, at the moment, it is difficult to falsify one model version over another, and to constrain nutrient effects on the variation of GPP, based on current observation-based GPP.

In order to further explore the underlying reasons of the general improvement in the IAV of GPP due to the inclusion of nutrient cycles, we analyzed the sensitivity of GPP anomalies to anomalies of

temperature (S_T), precipitation (S_P) and shortwave radiation (S_R), all with mean annual values (Sect. S1I in supplement). We found that S_P by ORCHIDEE-CNP compares well with BESS-GPP and MTE-GPP, while it is overestimated in ORCHIDEE (Figs. S7 and S8). Thus, the difference in S_P is likely the major reason for the differences in IAV in NH between model versions, as S_T and S_R show only minor differences there. This provides confidence that the improvement of IAV of GPP in the NH is due an improved sensitivity towards a climatic driver (i.e. S_P). For tropical regions, ORCHIDEE-CNP simulates more realistic S_P but higher biases in S_R than in ORCHIDEE, while observation based estimates of S_T disagree on the sign and model versions show only minor differences (Fig. S7). Therefore, the deterioration of the IAV of tropical GPP by the inclusion of nutrient cycles is likely caused by enhanced biases in S_R due to a lowering of LUE of GPP (Sect. 4.2 and 5.1).

5.5.2 Inclusion of nutrient cycling deteriorates phenology and on seasonality of GPP

The performance in reproducing seasonal variations of GPP was deteriorated by the inclusion of N and P nutrient cycles in ORCHIDEE (Fig. 10b). We found that biases in GPP are related to biases in the seasonality of the LAI introduced in ORCHIDEE-CNP (Figs. S9a and S10a). For NH, the delayed increase in LAI in ORCHIDEE-CNP could be partly caused by nutrient shortage during the first half of the growing season, as indicated by the increasing leaf nutrient concentration throughout the growing season (Fig. S11). Several factors could lead to a too low supply of nutrients in the beginning of the growing season: an insufficient internal plant nutrient reserve due to a too low resorption of nutrients prior to leaf shedding or an underestimation of nutrient uptake during the dormant season, an insufficient investment into root growth to acquire nutrients, and an overestimation of soil nutrient losses during dormant season leaving the soil nutrient depleted at the beginning of the growing season. Many of the related processes (e.g. root phenology, mineralization, nutrient resorption, growth allocation) are only rudimentary represented. For tropical regions, ORCHIDEE-CNP simulates a quasi-flat seasonal cycle of GPP, in contrast with a peak of GPP during the wet season in MTE-GPP and BESS-GPP, which is correctly captured by ORCHIDEE (Fig. S9b, c). The reduction of seasonal GPP in ORCHIDEE-CNP compared to ORCHIDEE is more pronounced in the dry season (~100 g C m^{-2}) than in the wet season (Fig. S9b, c), concurrent with a larger reduction of LAI in the dry season (Fig. S10b, c). Tropical phenology is currently only rudimentary represented in ORCHIDEE(-CNP) (Chen et al., 2020) causing a suboptimal allocation of nutrients to leaves which could cause the biases in the seasonal cycle of GPP and LAI. Model-data assimilation of phenology (Williams et al., 2009; MacBean et al., 2018; Bacour et al., 2019) and efforts to better characterize processes related to plant resource investment into different tissues and symbioses (Prentice et al., 2015; Warren et al., 2015; Jiang et al., 2019) and leaf age effects during the year for evergreen forests (Chen et al., 2020) should help to reduce tropical phenology biases in future versions of ORCHIDEE-CNP.

5.5.3 Inclusion of nutrient cycling leads to an underestimation of the land carbon sink

Current LSM unanimously conclude that CO_2 fertilization is the main driver of the land carbon sink and its trend (Friedlingstein et al., 2014), but it remains unclear to what extent other drivers (i.e. climate change, land management, nutrient deposition) contribute to the sink as well. Also, it remains unclear how commonly omitted dynamics (climate and management induced effects on tree mortality, nutrients)

lead to overestimation of the contribution of CO_2 fertilization in models (Ellsworth et al., 2017; Fleischer et al., 2019). ORCHIDEE-CNP simulates a land carbon sink over the past decades that is lower than other DGVM models and atmospheric inversions (Fig. S12), despite the fact that the response of GPP to CO_2 in ORCHIDEE-CNP is in line with proxy data (Fig. 5; Sect. 5.2). In particular, the NH carbon sink which persistently increased over the last 50 years (Ciais et al., 2019) is strongly underestimated. The few Free Air Carbon Enrichment (FACE) studies that have experimentally applied elevated CO_2 levels in mature stands found no increase in biomass production (Bader et al., 2013; Klein et al., 2016; Körner et al., 2005; Sigurdsson et al., 2013; Ellsworth et al., 2017), thus an increase in GPP does not necessarily translate into an increase in biomass production, whereas in most DGVMs where mortality is constant and growth follows GPP, biomass production is inevitably coupled to GPP. Based on upscaling of data from FACE experiments, Terrer et al. (2019) suggested that the effect of elevated CO_2 on biomass may be severely overestimated (on average by a factor of 3.6) in LSMs which ignore nutrients. It would be tempting to conclude from this study that ORCHIDEE-CNP is 'right' in its underestimation of the carbon sink whereas other models are 'wrong' because they miss processes such as forest regrowth (Pugh et al., 2019) from e.g. decreased harvesting pressure (Ciais et al., 2008) and thus have a realistic NH land sink for the wrong reasons. We also showed that ORCHIDEE-CNP underestimates peak GPP (Fig. S12b) and overestimates P limitations in the NH (Sect. 5.1, 5.3 and 5.4) thus, another explanation is that the NH sink in this study is too low because of too strong P limitations in this region. These two hypotheses explaining why we underestimate the NH sink (missing forest regrowth vs. too strong nutrient limitations in the NH) are examined below.

The too small NH carbon sink in ORCHIDEE-CNP may be explained by a too strong immobilization of nutrients in accumulating nutrient-rich organic matter, which leads to a reduction of plant available nutrients, the so-called 'progressive nutrient limitation' proposed by Luo et al. (2004) and subsequently to a reduced biomass production. The amount of accumulated N and P immobilized into SOM in the NH during 1850-2016 reaches up to 75.3 g N m^{-2} and 2.4 g P m^{-2} respectively, which is twice as much as the accumulated respective nutrient inputs to ecosystems in this region during the same period (37.8 g N m^{-2} and 1.6 g P m^{-2}; Figs. S13 and S14). This suggests a strong progressive nutrient limitation in the model. The omission of nutrient controls on litter and SOM decomposition in the soil module of ORCHIDEE-CNP could have favored the immobilization of nutrients in accumulating SOM (Zhang et al., 2018). Microbe incubation and N fertilization experiments showed that a low availability of nutrients can hamper the built-up of SOM as more carbon gets respired by decomposers due to an elevated energetic requirements of processing low quality substrate (Recous et al., 1995; Janssens et al., 2010; Allison et al., 2009) and an overall lower microbial activity (Wang et al., 2011; Knorr et al., 2005). Uncertainties with respect to the capability of ecosystems to up-regulate P mineralization when P becomes scarce could have contributed to the decline in plant available nutrients with increasing SOM stocks. The inclusion of nutrient effects on decomposition and microbial dynamics in ORCHIDEE-CNP is ongoing (Zhang et al., 2018, 2020) but the lack of a quantification of the ability of ecosystems to enhance P recycling hampers model developments.

The too small NH carbon sink in ORCHIDEE-CNP may also be explained by the lack of representation of effects of forest age and management on biomass turnover and biomass production efficiency (i.e. CUE). Pugh et al. (2019) found that old-growth forests in the NH have a much smaller C sink than re-

growing forests (<0.1 Pg C yr^{-1} compared to 0.86 Pg C yr^{-1}) for the period 2001-2010. Forest management effects on biomass production efficiency and biomass turnover is only rudimentary represented in ORCHIDEE(-CNP). ORCHIDEE-CNP prescribes constant tree mortality rates (i.e. the fraction of total carbon in wood lost to litter) whereas in reality tree mortality rates change with management and climate conditions (Peng et al., 2011). Moreover, ORCHIDEE(-CNP) omits the effect of forest age on C uptake. Compared to data-driven estimates for C storage (Sect. S1G and S1H in supplement), ORCHIDEE-CNP simulates a higher global aboveground forest biomass (387 Pg C; 283 Pg C for GlobBiomass and 221 Pg C for GEOCARBON; Fig. S2) but lower global soil organic carbon (801 Pg C; 4387 Pg C for Soilgrids and 1680 Pg C for GSDE; Fig. S3).

6 Concluding remarks

In this study, we evaluated the performance of ORCHIDEE-CNP and found that the model has sufficient skills in capturing observed patterns in 1) vegetation resource use efficiencies, 2) CO_2 vegetation fertilization, 3) ecosystem N and P openness and turnover and 4) leaf and soil stoichiometry. The inclusion of nutrients improves the simulation of the sensitivity of plant productivity to increasing CO_2 and to inter-annual variation in precipitation. However, the nutrient-enabled version cannot capture the current land carbon sink in the NH. This suggests that either the land carbon sink might be less a consequence of the CO_2 fertilization effect, but of other processes that are currently not well resolved in global models (e.g. biomass turnover, land management), or that ORCHIDEE-CNP underestimates the ability of ecosystems to circumpass nutrient constraints on biomass built up under elevated CO_2. We propose the following focus to improve ORCHIDEE in next model versions: 1) refine the canopy light absorption processes; 2) use model-data assimilation frameworks (like ORCHIDAS) to better calibrate root phenology, mineralization, nutrient resorption and growth allocation; 3) better represent soil processes related to decomposition, stabilization of soil organic matter (e.g. Zhang et al., 2018, 2020) and inorganic P transformation (e.g. Helfenstein et al., 2020); 4) refine dynamics of biomass turnover and biomass production efficiency including effects of forest management and climate. Continued improvements of nutrient cycle representations will further reduce uncertainties in predicting land carbon sink under climate change and rising atmospheric CO_2.

Code and data availability

The source code is freely available online via the following address: http://forge.ipsl.jussieu.fr/orchidee/wiki/GroupActivities/CodeAvalaibilityPublication/ORCHIDEE-CN-P_v1.2_r5986 (Goll, 2020). Please contact the corresponding author if you plan an application of the model and envisage longer-term scientific collaboration.

Primary data and scripts used in the analysis and other supplementary information that may be useful in reproducing the author's work can be obtained by http://dx.doi.org/10.17632/f54v9zcgbf.1

Supplement. The supplement related to this article is available online at: (a doi will be provided before final publication).

Author contributions. YS and DSG carried out the simulation of ORCHIDEE-CNP. YS, JC, JH, VN, YW and HY analyzed the model outputs. YS, DSG, and PC prepared the paper with contributions from all coauthors.

Competing interests. The authors declare that they have no conflict of interest.

Acknowledgements. YS, DSG, PC, HZ and YH are funded by the IMBALANCE-P project of the European Research Council (ERC-2013-SyG610028). JH is supported by the Swiss National Science Foundation (Project number 200021_162422).

References

Ågren, G. I.: Stoichiometry and nutrition of plant growth in natural communities, Annu. Rev. Ecol. Evol. Syst., 39, 153-170, http://doi.org/10.1146/annurev.ecolsys.39.110707.173515, 2008.

Albert, L. P., Wu, J., Prohaska, N., de Camargo, P. B., Huxman, T. E., Tribuzy, E. S., Ivanov, V. Y., Oliveira, R. S., Garcia, S., Smith, M. N., Oliveira, R.C., Restrepo-Coupe, N., da Silva, R., Stark, S.C., Martins, G.A., Penha, D.V., and Saleska, S.R.: Age-dependent leaf physiology and consequences for crown-scale carbon uptake during the dry season in an Amazon evergreen forest, New Phytol., 218, 870-884, http://doi.org/10.1111/nph.15056, 2018.

Allen Jr, L. H.: Carbon dioxide increase: Direct impacts on crops and indirect effects mediated through anticipated climatic changes, Physiology and determination of crop yield, 425-459, 1994.

Allison, S. D., LeBauer, D. S., Ofrecio, M. R., Reyes, R., Ta, A.-M., and Tran, T. M.: Low levels of nitrogen addition stimulate decomposition by boreal forest fungi, Soil Biol. Biochem., 41, 293-302, http://doi.org/10.1016/j.soilbio.2008.10.032, 2009.

Anav, A., Friedlingstein, P., Beer, C., Ciais, P., Harper, A., Jones, C., Murray‐Tortarolo, G., Papale, D., Parazoo, N. C., Peylin, P., Piao, S., Sitch, S., Viovy, N., Wiltshire, A., and Zhao, M.: Spatiotemporal patterns of terrestrial gross primary production: A review, Rev. Geophys., 53, 785-818, http://doi.org/10.1002/2015RG000483, 2015.

Baccini, A., Goetz, S., Walker, W., Laporte, N., Sun, M., Sulla-Menashe, D., Hackler, J., Beck, P., Dubayah, R., Friedl, M., Samanta, S., and Houghton, R.: Estimated carbon dioxide emissions from tropical deforestation improved by carbon-density maps, Nat. Clim. Chang., 2, 182-185, http://doi.org/10.1038/nclimate1354, 2012.

Bacour, C., Maignan, F., Peylin, P., MacBean, N., Bastrikov, V., Joiner, J., Köhler, P., Guanter, L., and Frankenberg, C.: Differences Between OCO‐2 and GOME‐2 SIF Products From a Model‐Data Fusion Perspective, J. Geophys. Res. Biogeosci., 124, 3143-3157, http://doi.org/10.1029/2018JG004938, 2019.

Bader, M. K. F., Leuzinger, S., Keel, S. G., Siegwolf, R. T., Hagedorn, F., Schleppi, P., and Körner, C.: Central European hardwood trees in a high‐CO2 future: synthesis of an 8‐year forest canopy CO2 enrichment project, J. Ecol., 101, 1509-1519, http://doi.org/10.1111/1365-2745.12149, 2013.

Baret, F., Weiss, M., Lacaze, R., Camacho, F., Makhmara, H., Pacholcyzk, P., and Smets, B.: GEOV1: LAI and FAPAR essential climate variables and FCOVER global time series capitalizing over existing products. Part1: Principles of development and production, Remote Sens. Environ., 137, 299-309, http://doi.org/10.1016/j.rse.2012.12.027, 2013.

Bodirsky, B., Popp, A., Weindl, I., Dietrich, J., Rolinski, S., Scheiffele, L., Schmitz, C., and Lotze-Campen, H.: N2O emissions from the global agricultural nitrogen cycle - current state and future scenarios, Biogeosciences, 9, 4169-4197, http://doi.org/10.5194/bg-9-4169-2012, 2012.

Bontemps, S., Defourny, P., Radoux, J., Van Bogaert, E., Lamarche, C., Achard, F., Mayaux, P., Boettcher, M., Brockmann, C., and Kirches, G.: Consistent global land cover maps for climate modelling communities: current achievements of the ESA's land cover CCI, Proceedings of the ESA Living Planet Symposium, Edimburgh, 2013, 9-13, 2013.

Bouwman, A., Beusen, A. H., and Billen, G.: Human alteration of the global nitrogen and phosphorus soil balances for the period 1970–2050, Glob. Biogeochem. Cycle, 23, http://doi.org/10.1029/2009GB003576, 2009.

Bouwman, A., Beusen, A., Griffioen, J., Van Groenigen, J., Hefting, M., Oenema, O., Van Puijenbroek, P., Seitzinger, S., Slomp, C., and Stehfest, E.: Global trends and uncertainties in terrestrial denitrification and N2O emissions, Philos. Trans. R. Soc. B-Biol. Sci., 368, http://doi.org/10.1098/rstb.2013.0112, 2013a.

Bouwman, L., Goldewijk, K. K., Van Der Hoek, K. W., Beusen, A. H., Van Vuuren, D. P., Willems, J., Rufino, M. C., and Stehfest, E.: Exploring global changes in nitrogen and phosphorus cycles in agriculture induced by livestock production over the 1900–2050 period, Proc. Natl. Acad. Sci. U. S. A., 110, 20882-20887, http://doi.org/10.1073/pnas.1012878108, 2013b.

Bowes, G.: Facing the inevitable: plants and increasing atmospheric CO2, Annu. Rev. Plant. Biol., 44, 309-332, http://doi.org/10.1146/annurev.arplant.44.1.309, 1993.

Brovkin, V., and Goll, D.: Land unlikely to become large carbon source, Nat. Geosci., 8, 893-893, http://doi.org/10.1038/ngeo2598, 2015.

Bünemann, E. K.: Assessment of gross and net mineralization rates of soil organic phosphorus–A review, Soil Biol. Biochem., 89, 82-98, http://doi.org/10.1016/j.soilbio.2015.06.026, 2015.

Butler, E. E., Datta, A., Flores-Moreno, H., Chen, M., Wythers, K. R., Fazayeli, F., Banerjee, A., Atkin, O. K., Kattge, J., Amiaud, B., Blonder, B., Boenisch, G., Bond-Lamberty, B., Brown, K. A., Byun, C., Campetella, G., Cerabolini, B. E. L., Cornelissen, J. H. C., Craine, J. M., Craven, D., de Vries, F. T., Díaz, S., Domingues, T. F., Forey, E., González-Melo, A., Gross, N., Han, W., Hattingh, W. N., Hickler, T., Jansen, S., Kramer, K., Kraft, N. J. B., Kurokawa, H., Laughlin, D. C., Meir, P., Minden, V., Niinemets, Ü., Onoda, Y., Peñuelas, J., Read, Q., Sack, L., Schamp, B., Soudzilovskaia, N. A.,

Spasojevic, M. J., Sosinski, E., Thornton, P. E., Valladares, F., van Bodegom, P. M., Williams, M., Wirth, C., and Reich, P. B.: Mapping local and global variability in plant trait distributions, Proc. Natl. Acad. Sci. U. S. A., 114, E10937-E10946, http://doi.org/10.1073/pnas.1708984114, 2017.

Butt, T. A., Phillips, I., Guan, L., and Oikonomou, G.: TRENDY: An adaptive and context-aware service discovery protocol for 6LoWPANs, Proceedings of the third international workshop on the web of things, 2012, 1-6,

Campbell, J., Berry, J., Seibt, U., Smith, S. J., Montzka, S., Launois, T., Belviso, S., Bopp, L., and Laine, M.: Large historical growth in global terrestrial gross primary production, Nature, 544, 84-87, http://doi.org/10.1038/nature22030, 2017.

Carvalhais, N., Forkel, M., Khomik, M., Bellarby, J., Jung, M., Migliavacca, M., Mu, M., Saatchi, S., Santoro, S., Thurner, M., Weber, U., Ahrens, B., Beer, C., Cescatti, A., Randerson, J. T., and Reichstein, M.: Global covariation of carbon turnover times with climate in terrestrial ecosystems, Nature, 514, 213–217, http://doi.org/10.1038/nature13731, 2014.

Chen, B., Coops, N. C., Andy Black, T., Jassal, R. S., Chen, J. M., and Johnson, M.: Modeling to discern nitrogen fertilization impacts on carbon sequestration in a Pacific Northwest Douglas‐fir forest in the first‐postfertilization year, Glob. Change Biol., 17, 1442-1460, http://doi.org/10.1111/j.1365-2486.2010.02298.x, 2011.

Chen, X., Maignan, F., Viovy, N., Bastos, A., Goll, D., Wu, J., Liu, L., Yue, C., Peng, S., and Yuan, W.: Novel representation of leaf phenology improves simulation of Amazonian evergreen forest photosynthesis in a land surface model, J. Adv. Model Earth Syst., 12, e2018MS001565, http://doi.org/10.1029/2018MS001565, 2020.

Chevallier, F., Fisher, M., Peylin, P., Serrar, S., Bousquet, P., Bréon, F. M., Chédin, A., and Ciais, P.: Inferring CO2 sources and sinks from satellite observations: Method and application to TOVS data, J. Geophys. Res.-Atmos., 110, http://doi.org/10.1029/2005JD006390, 2005.

Ciais, P., Schelhaas, M.-J., Zaehle, S., Piao, S., Cescatti, A., Liski, J., Luyssaert, S., Le-Maire, G., Schulze, E.-D., Bouriaud, O., Freibauer, A., Valentini, R., and Nabuurs, G. J.: Carbon accumulation in European forests, Nature, 1, 425-429, http://doi.org/10.1038/ngeo233, 2008.

Ciais, P., Tan, J., Wang, X., Roedenbeck, C., Chevallier, F., Piao, S.-L., Moriarty, R., Broquet, G., Le Quéré, C., and Canadell, J., Peng, S., Poulter, B., Liu, Z., and Tans, P.: Five decades of northern land carbon uptake revealed by the interhemispheric CO2 gradient, Nature, 568, 221-225, http://doi.org/10.1038/s41586-019-1078-6, 2019.

Cleveland, C. C., Houlton, B. Z., Smith, W. K., Marklein, A. R., Reed, S. C., Parton, W., Del Grosso, S. J., and Running, S. W.: Patterns of new versus recycled primary production in the terrestrial biosphere, Proc. Natl. Acad. Sci. U. S. A., 110, 12733-12737, http://doi.org/10.1073/pnas.1302768110, 2013.

Conant, R. T., Berdanier, A. B., and Grace, P. R.: Patterns and trends in nitrogen use and nitrogen recovery efficiency in world agriculture, Global Biogeochem. Cycles, 27, 558-566, http://doi.org/10.1002/gbc.20053, 2013.

D'Odorico, P., Gonsamo, A., Pinty, B., Gobron, N., Coops, N., Mendez, E., and Schaepman, M. E.: Intercomparison of fraction of absorbed photosynthetically active radiation products derived from satellite data over Europe, Remote Sens. Environ., 142, 141-154, http://doi.org/10.1016/j.rse.2013.12.005, 2014.

Du, E., Terrer, C., Pellegrini, A. F., Ahlström, A., van Lissa, C. J., Zhao, X., Xia, N., Wu, X., and Jackson, R. B.: Global patterns of terrestrial nitrogen and phosphorus limitation, Nat. Geosci., 13, 221-226, http://doi.org/10.1038/s41561-019-0530-4, 2020.

Ehlers, I., Augusti, A., Betson, T. R., Nilsson, M. B., Marshall, J. D., and Schleucher, J.: Detecting long-term metabolic shifts using isotopomers: CO2-driven suppression of photorespiration in C3 plants over the 20th century, Proc. Natl. Acad. Sci. U. S. A., 112, 15585-15590, http://doi.org/10.1073/pnas.1504493112, 2015.

Ellsworth, D. S., Anderson, I. C., Crous, K. Y., Cooke, J., Drake, J. E., Gherlenda, A. N., Gimeno, T. E., Macdonald, C. A., Medlyn, B. E., Powell, J. R., Tjoelker, M. G., and Reich, P. B.: Elevated CO2 does not increase eucalypt forest productivity on a low-phosphorus soil, Nat. Clim. Chang., 7, 279-282, http://doi.org/10.1038/nclimate3235, 2017.

Elser, J. J., Bracken, M. E., Cleland, E. E., Gruner, D. S., Harpole, W. S., Hillebrand, H., Ngai, J. T., Seabloom, E. W., Shurin, J. B., and Smith, J. E.: Global analysis of nitrogen and phosphorus limitation of primary producers in freshwater, marine and terrestrial ecosystems, Ecol. Lett., 10, 1135-1142, http://doi.org/10.1111/j.1461-0248.2007.01113.x, 2007.

Esser, G., Kattge, J., and Sakalli, A.: Feedback of carbon and nitrogen cycles enhances carbon sequestration in the terrestrial biosphere, Glob. Change Biol., 17, 819-842, http://doi.org/10.1111/j.1365-2486.2010.02261.x, 2011.

Fardeau, J., Morel, C., and Boniface, R.: Phosphate ion transfer from soil to soil solution: kinetic parameters [available P, phosphate flow], Agronomie, http://doi.org/10.1051/agro:19910909, 1991.

Fernández-Martínez, M., Vicca, S., Janssens, I. A., Sardans, J., Luyssaert, S., Campioli, M., Chapin III, F. S., Ciais, P., Malhi, Y., Obersteiner, M., Papale, D., Piao, S. L., Reichstein, M., Rodà, F., and Peñuelas, J.: Nutrient availability as the key regulator of global forest carbon balance, Nat. Clim. Chang., 4, 471-476, http://doi.org/10.1038/nclimate2177, 2014.

Fleischer, K., Rammig, A., De Kauwe, M. G., Walker, A. P., Domingues, T. F., Fuchslueger, L., Garcia, S., Goll, D. S., Grandis, A., Jiang, M., Haverd, V., Hofhansl, F., Holm, J. A., Kruijt, B., Leung, F., Medlyn, B. E., Mercado, L. M., Norby, R. J., Pak, B., von Randow, C., Quesada, C. A., Schaap, K. J., Valverde-Barrantes, O. J., Wang, Y., Yang, X., Zaehle, S., Zhu, Q., and Lapola, D. M.: Amazon forest response to CO2 fertilization dependent on plant phosphorus acquisition, Nat. Geosci., 12, 736-741, http://doi.org/10.1038/s41561-019-0404-9, 2019.

Freschet, G. T., Cornelissen, J. H., Van Logtestijn, R. S., and Aerts, R.: Evidence of the 'plant economics spectrum'in a subarctic flora, J. Ecol., 98, 362-373, http://doi.org/10.1111/j.1365-2745.2009.01615.x, 2010.

Friedlingstein, P., Meinshausen, M., Arora, V. K., Jones, C. D., Anav, A., Liddicoat, S. K., and Knutti, R.: Uncertainties in CMIP5 climate projections due to carbon cycle feedbacks, J. Clim., 27, 511-526, http://doi.org/10.1175/JCLI-D-12-00579.1, 2014.

Friedlingstein, P., Jones, M. W., O'Sullivan, M., Andrew, R. M., Hauck, J., Peters, G. P., Peters, W., Pongratz, J., Sitch, S., Le Quéré, C., Bakker, D. C. E., Canadell, J. G., Ciais, P., Jack- son, R. B., Anthoni, P., Barbero, L., Bastos, A., Bastrikov, V., Becker, M., Bopp, L., Buitenhuis, E., Chandra, N., Chevallier, F., Chini, L. P., Currie, K. I., Feely, R. A., Gehlen, M., Gilfillan, D., Gkritzalis, T., Goll, D. S., Gruber, N., Gutekunst, S., Har- ris, I., Haverd, V., Houghton, R. A., Hurtt, G., Ilyina, T., Jain, A. K., Joetzjer, E., Kaplan, J. O., Kato, E., Klein Goldewijk, K., Korsbakken, J. I., Landschützer, P., Lauvset, S. K., Lefèvre, N., Lenton, A., Lienert, S., Lombardozzi, D., Marland, G., McGuire, P. C., Melton, J. R., Metzl, N., Munro, D. R., Nabel, J. E. M. S., Nakaoka, S.-I., Neill, C., Omar, A. M., Ono, T., Peregon, A., Pierrot, D., Poulter, B., Rehder, G., Resplandy, L., Robertson, E., Rödenbeck, C., Séférian, R., Schwinger, J., Smith, N., Tans, P. P., Tian, H., Tilbrook, B., Tubiello, F. N., van der Werf, G. R., Wiltshire, A. J., and Zaehle, S.: Global Carbon Budget 2019, Earth Syst. Sci. Data, 11, 1783–1838, https://doi.org/10.5194/essd-11- 1783-2019, 2019.

Frossard, E., Achat, D. L., Bernasconi, S. M., Bünemann, E. K., Fardeau, J.-C., Jansa, J., Morel, C., Rabeharisoa, L., Randriamanantsoa, L., Sinaj, S., Tamburini, F., and Oberson, A.: The use of tracers to investigate phosphate cycling in soil–plant systems, in: Phosphorus in Action, Springer, 59-91, 2011.

Galloway, J. N., Dentener, F. J., Capone, D. G., Boyer, E. W., Howarth, R. W., Seitzinger, S. P., Asner, G. P., Cleveland, C. C., Green, P., Holland, E. A. Karl, D. M., Michaels, A. F., Porter, J. H., Townsend, A. R., Vöosmarty, C. J.: Nitrogen cycles: past, present, and future, Biogeochemistry, 70, 153-226, http://doi.org/10.1007/s10533-004-0370-0, 2004.

Gärdenäs, A. I., Ågren, G. I., Bird, J. A., Clarholm, M., Hallin, S., Ineson, P., Kätterer, T., Knicker, H., Nilsson, S. I., Näsholm, T., Ogle, S., Paustian, K., Persson, T., Stendahl, J.: Knowledge gaps in soil carbon and nitrogen interactions–from molecular to global scale, Soil Biol. Biochem., 43, 702-717, http://doi.org/10.1016/j.soilbio.2010.04.006, 2011.

Garrigues, S., Lacaze, R., Baret, F., Morisette, J., Weiss, M., Nickeson, J., Fernandes, R., Plummer, S., Shabanov, N., Myneni, R., Knyazikhin, Y., Yang, W.: Validation and intercomparison of global Leaf Area Index products derived from remote sensing data, J. Geophys. Res.-Biogeosci., 113, http://doi.org/10.1029/2007JG000635, 2008.

Gill, A. L., and Finzi, A. C.: Belowground carbon flux links biogeochemical cycles and resource‐use efficiency at the global scale, Ecol. Lett., 19, 1419-1428, http://doi.org/10.1111/ele.12690, 2016.

Gobron, N., Pinty, B., Aussedat, O., Chen, J., Cohen, W. B., Fensholt, R., Gond, V., Huemmrich, K. F., Lavergne, T., Mélin, F., Privette, J. L., Sandholt, I., Taberner, M., Turner, D. P., Verstraete, M. M., and Widlowski, J.: Evaluation of fraction of absorbed photosynthetically active radiation products for different canopy radiation transfer regimes: Methodology and results using Joint Research Center products derived from SeaWiFS against ground-based estimations, J. Geophys. Res.-Atmos, 111, D13110, http://doi.org/10.1029/2005JD006511, 2006a.

Gobron, N., Pinty, B., Taberner, M., Mélin, F., Verstraete, M., and Widlowski, J.-L.: Monitoring the photosynthetic activity of vegetation from remote sensing data, Adv. Space Res., 38, 2196-2202, http://doi.org/10.1016/j.asr.2003.07.079, 2006b.

Goll, D. S., Brovkin, V., Parida, B., Reick, C. H., Kattge, J., Reich, P. B., Van Bodegom, P., and Niinemets, Ü.: Nutrient limitation reduces land carbon uptake in simulations with a model of combined carbon, nitrogen and phosphorus cycling, Biogeosciences, 9, 3547-3569, http://doi.org/10.5194/bg-9-3547-2012, 2012.

Goll, D., Vuichard, N., Maignan, F., Jornet-Puig, A., Sardans, J., Violette, A., Peng, S., Sun, Y., Kvakic, M., and Guimberteau, M.: A representation of the phosphorus cycle for ORCHIDEE (revision 4520), Geosci. Model Dev., 10, 3745-3770, http://doi.org/10.5194/gmd-10-3745-2017, 2017a.

Goll, D. S., Winkler, A. J., Raddatz, T., Dong, N., Prentice, I. C., Ciais, P., and Brovkin, V.: Carbon-nitrogen interactions in idealized simulations with JSBACH (version 3.10), Geosci. Model Dev., 10, 2009-2030, http://doi.org/10.5194/gmd-10-2009-2017, 2017b.

Goll, D. S., Joetzjer, E., Huang, M., and Ciais, P.: Low phosphorus availability decreases susceptibility of tropical primary productivity to droughts, Geophys. Res. Lett., 45, 8231-8240, http://doi.org/10.1029/2018GL077736, 2018.

Güsewell, S.: N: P ratios in terrestrial plants: variation and functional significance, New Phytol., 164, 243-266, http://doi.org/10.1111/j.1469-8137.2004.01192.x, 2004.

Harris, I., Jones, P. D., Osborn, T. J., and Lister, D. H.: Updated high‐resolution grids of monthly climatic observations‐the CRU TS3. 10 Dataset, Int. J. Climatol., 34, 623-642, http://doi.org/10.1002/joc.3711, 2014.

Hartmann, J., and Moosdorf, N.: The new global lithological map database GLiM: A representation of rock properties at the Earth surface, Geochem. Geophys. Geosyst., 13, http://doi.org/10.1029/2012GC004370, 2012.

Hartmann, J., Moosdorf, N., Lauerwald, R., Hinderer, M., and West, A. J.: Global chemical weathering and associated P-release—The role of lithology, temperature and soil properties, Chem. Geol., 363, 145-163, http://doi.org/10.1016/j.chemgeo.2013.10.025, 2014.

He, Y., Piao, S., Li, X., Chen, A., and Qin, D.: Global patterns of vegetation carbon use efficiency and their climate drivers deduced from MODIS satellite data and process-based models, Agric. For. Meteorol., 256, 150-158, http://doi.org/10.1016/j.agrformet.2018.03.009, 2018.

Helfenstein, J., Jegminat, J., McLaren, T. I., and Frossard, E.: Soil solution phosphorus turnover: derivation, interpretation, and insights from a global compilation of isotope exchange kinetic studies, Biogeosciences, 15, 105-114, http://doi.org/10.5194/bg-15-105-2018, 2018.

Helfenstein, J., Pistocchi, C., Oberson, A., Tamburini, F., Goll, D. S., and Frossard, E.: Estimates of mean residence times of phosphorus in commonly considered inorganic soil phosphorus pools, Biogeosciences, 17, 441-454, http://doi.org/10.5194/bg-17-441-2020, 2020.

Hengl, T., de Jesus, J. M., MacMillan, R. A., Batjes, N. H., Heuvelink, G. B., Ribeiro, E., Samuel-Rosa, A., Kempen, B., Leenaars, J. G., Walsh, M. G. Gonzalez, M. R.: SoilGrids1km—global soil information based on automated mapping, PLoS One, 9, http://doi.org/10.1371/journal.pone.0105992, 2014.

Hodapp, D., Hillebrand, H., and Striebel, M.: "Unifying" the concept of resource use efficiency in ecology, Front. Ecol. Evol., 6, 233, http://doi.org/10.3389/fevo.2018.00233, 2019.

Houlton, B. Z., Wang, Y.-P., Vitousek, P. M., and Field, C. B.: A unifying framework for dinitrogen fixation in the terrestrial biosphere, Nature, 454, 327-330, http://doi.org/10.1038/nature07028, 2008.

Hungate, B. A., Dukes, J. S., Shaw, M. R., Luo, Y., and Field, C. B.: Nitrogen and climate change, Science, 302, 1512-1513, http://doi.org/10.1126/science.1091390, 2003.

Huntzinger, D. N., Michalak, A., Schwalm, C., Ciais, P., King, A., Fang, Y., Schaefer, K., Wei, Y., Cook, R., Fisher, J., Hayes, D., Huang, M., Ito, A., Jain, A. K., Lei, H., Lu, C., Maignan, F., Mao, J., Parazoo, N., Peng, S., Poulter, B., Ricciuto, D., Shi, X., Tian, H., Wang, W., Zeng, N., and Zhao, F.: Uncertainty in the response of terrestrial carbon sink to environmental drivers undermines carbon-climate feedback predictions, Sci. Rep., 7, 1-8, http://doi.org/10.1038/s41598-017-03818-2, 2017.

Hurtt, G. C., Chini, L. P., Frolking, S., Betts, R. A., Feddema, J., Fischer, G., Fisk, J. P., Hibbard, K., Houghton, R. A., Janetos, A., Jones, C. D., Kindermann, G., Kinoshita, T., Klein Gold- ewijk, K., Riahi, K., Shevliakova, E., Smith, S., Stehfest, E., Thomson, A., Thornton, P., van Vuuren, D. P., and Wang, Y. P.: Harmonization of land-use scenarios for the period 1500–2100: 600 years of global gridded annual land-use transitions, wood harvest, and resulting secondary lands, Climatic Change, 109, 117–161, http://doi.org/10.1007/s10584-011-0153-2, 2011.

Ishida, A., Diloksumpun, S., Ladpala, P., Staporn, D., Panuthai, S., Gamo, M., Yazaki, K., Ishizuka, M., and Puangchit, L.: Contrasting seasonal leaf habits of canopy trees between tropical dry-deciduous and evergreen forests in Thailand, Tree Physiol., 26, 643-656, http://doi.org/10.1093/treephys/26.5.643, 2006.

Ito, A., and Oikawa, T.: Global mapping of terrestrial primary productivity and light-use efficiency with a process-based model, Global Environmental Change in the Ocean and on Land, 343-358, 2004.

Janssens, I. A., and Vicca, S.: Soil carbon breakdown, Nat. Geosci., 3, 823-824, http://doi.org/10.1038/ngeo1024, 2010.

Jiang, C., and Ryu, Y.: Multi-scale evaluation of global gross primary productivity and evapotranspiration products derived from Breathing Earth System Simulator (BESS), Remote Sens. Environ., 186, 528-547, http://doi.org/10.1016/j.rse.2016.08.030, 2016.

Jiang, M., Caldararu, S., Zaehle, S., Ellsworth, D. S., and Medlyn, B. E.: Towards a more physiological representation of vegetation phosphorus processes in land surface models, New Phytol., 222, 1223-1229, http://doi.org/10.1111/nph.15688, 2019.

Jung, M., Reichstein, M., and Bondeau, A.: Towards global empirical upscaling of FLUXNET eddy covariance observations: validation of a model tree ensemble approach using a biosphere model, Biogeosciences, http://doi.org/10.5194/bg-6-2001-2009, 2009.

Jung, M., Reichstein, M., Margolis, H. A., Cescatti, A., Richardson, A. D., Arain, M. A., Arneth, A., Bernhofer, C., Bonal, D., Chen, J., Damiano, G., Gobron, N., Kiely, G., Kutsch, W., Lasslop, G., Law, B. E., Lindroth, A., Merbold, L., Montagnani, L., Moors, E. J., Papale, D., Sottocornola, M., Vaccari, F., and Williams, C.: Global patterns of land-atmosphere fluxes of carbon dioxide, la- tent heat, and sensible heat derived from eddy covariance, satel- lite, and meteorological observations, J. Geophys. Res.-Biogeo., 116, http://doi.org/10.1029/2010JG001566, 2011.

Kattge, J., Knorr, W., Raddatz, T., and Wirth, C.: Quantifying photosynthetic capacity and its relationship to leaf nitrogen content for global‐scale terrestrial biosphere models, Glob. Change Biol., 15, 976-991, http://doi.org/10.1111/j.1365-2486.2008.01744.x, 2009.

Kerkhoff, A. J., Enquist, B. J., Elser, J. J., and Fagan, W. F.: Plant allometry, stoichiometry and the temperature‐dependence of primary productivity, Glob. Ecol. Biogeogr., 14, 585-598, http://doi.org/10.1111/j.1466-822x.2005.00187.x, 2005.

Kimball, B., and Idso, S.: Increasing atmospheric CO2: effects on crop yield, water use and climate, Agric. Water Manage., 7, 55-72, http://doi.org/10.1016/0378-3774(83)90075-6, 1983.

Klein Goldewijk, K., Beusen, A., Doelman, J., and Stehfest, E.: Anthropogenic land use estimates for the Holocene – HYDE 3.2, Earth Syst. Sci. Data, 9, 927-953, http://doi.org/10.5194/essd-9-927-2017, 2017a.

Klein Goldewijk, K., Dekker, S. C., and van Zanden, J. L.: Per-capita estimations of long-term historical land use and the consequences for global change research, J. Land Use Sci., 12, 313-337, http://doi.org/10.1080/1747423X.2017.1354938, 2017b.

Klein, T., Siegwolf, R. T., and Körner, C.: Belowground carbon trade among tall trees in a temperate forest, Science, 352, 342-344, http://doi.org/10.1126/science.aad6188, 2016.

Knorr, M., Frey, S., and Curtis, P.: Nitrogen additions and litter decomposition: A meta‐analysis, Ecology, 86, 3252-3257, http://doi.org/10.1890/05-0150, 2005.

Kobayashi, S., Ota, Y., Harada, Y., Ebita, A., Moriya, M., Onoda, H., Onogi, K., Kamahori, H., Kobayashi, C., Endo, H., Miyaoka, K., and Takahashi, K.: The JRA-55 Reanalysis: General Specifications and Basic Characteristics, J. Meteorol. Soc. Jpn, Ser. II, 93, 5–48, https://doi.org/10.2151/jmsj.2015-001, 2015.

Körner, C., Asshoff, R., Bignucolo, O., Hättenschwiler, S., Keel, S. G., Peláez-Riedl, S., Pepin, S., Siegwolf, R. T., and Zotz, G.: Carbon flux and growth in mature deciduous forest trees exposed to elevated CO2, Science, 309, 1360-1362, http://doi.org/10.1126/science.1113977, 2005.

Krinner, G., Viovy, N., de Noblet‐Ducoudré, N., Ogée, J., Polcher, J., Friedlingstein, P., Ciais, P., Sitch, S., and Prentice, I. C.: A dynamic global vegetation model for studies of the coupled atmosphere‐biosphere system, Glob. Biogeochem. Cycle, 19, http://doi.org/10.1029/2003GB002199, 2005.

Kvakić, M., Tzagkarakis, G., Pellerin, S., Ciais, P., Goll, D., Mollier, A., and Ringeval, B.: Carbon and phosphorus allocation in annual plants: an optimal functioning approach, Front. Plant Sci., 11, http://doi.org/10.3389/fpls.2020.00149, 2020.

Lassaletta, L., Billen, G., Grizzetti, B., Anglade, J., and Garnier, J.: 50 year trends in nitrogen use efficiency of world cropping systems: the relationship between yield and nitrogen input to cropland, Environ. Res. Lett., 9, 105011, http://doi.org/10.1088/1748-9326/9/10/105011, 2014.

Le Maire, G., Delpierre, N., Jung, M., Ciais, P., Reichstein, M., Viovy, N., Granier, A., Ibrom, A., Kolari, P., Longdoz, B., Moors, E. J., Pilegaard, K., Rambal, S., Richardson, A. D., and Vesala, T.: Detecting the critical periods that underpin interannual fluctuations in the carbon balance of European forests, J. Geophys. Res., 115, G00H03, http://doi.org/10.1029/2009JG001244, 2010.

Le Quéré, C., Andrew, R. M., Friedlingstein, P., Sitch, S., Hauck, J., Pongratz, J., Pickers, P. A., Korsbakken, J. I., Peters, G. P., Canadell, J. G., Arneth, A., Arora, V. K., Barbero, L., Bastos, A., Bopp, L., Chevallier, F., Chini, L. P., Ciais, P., Doney, S. C., Gkritzalis, T., Goll, D. S., Harris, I., Haverd, V., Hoffman, F. M., Hoppema, M., Houghton, R. A., Hurtt, G., Ilyina, T., Jain, A. K., Johannessen, T., Jones, C. D., Kato, E., Keeling, R. F., Gold- ewijk, K. K., Landschützer, P., Lefèvre, N., Lienert, S., Liu, Z., Lombardozzi, D., Metzl, N., Munro, D. R., Nabel, J. E. M. S., Nakaoka, S., Neill, C., Olsen, A., Ono, T., Patra, P., Peregon, A., Peters, W., Peylin, P., Pfeil, B., Pierrot, D., Poulter, B., Re- hder, G., Resplandy, L., Robertson, E., Rocher, M., Rödenbeck, C., Schuster, U., Schwinger, J., Séférian, R., Skjelvan, I., Stein- hoff, T., Sutton, A., Tans, P. P., Tian, H., Tilbrook, B., Tubiello, F. N., van der Laan-Luijkx, I. T., van der Werf, G. R., Viovy, N., Walker, A. P., Wiltshire, A. J., Wright, R., Zaehle, S., and Zheng, B.: Global Carbon Budget 2018, Earth Syst. Sci. Data, 10, 2141– 2194, https://doi.org/10.5194/essd-10-2141-2018, 2018.

Liu, W., Yang, H., Ciais, P., Stamm, C., Zhao, X., Williams, J. R., Abbaspour, K. C., and Schulin, R.: Integrative Crop‐Soil‐Management Modeling to Assess Global Phosphorus Losses from Major Crop Cultivations, Glob. Biogeochem. Cycle, 32, 1074-1086, http://doi.org/10.1029/2017GB005849, 2018.

Liu, Y., Piao, S., Gasser, T., Ciais, P., Yang, H., Wang, H., Keenan, T. F., Huang, M., Wan, S., and Song, J.: Field-experiment constraints on the enhancement of the terrestrial carbon sink by CO2 fertilization, Nat. Geosci., 12, 809-814, http://doi.org/10.1038/s41561-019-0436-1, 2019.

Lu, C. C., and Tian, H.: Global nitrogen and phosphorus fertilizer use for agriculture production in the past half century: shifted hot spots and nutrient imbalance, Earth Syst. Sci. Data, 9, 181, http://doi.org/10.5194/essd-9-181-2017, 2017.

Lun, F., Liu, J., Ciais, P., Nesme, T., Chang, J., Wang, R., Goll, D., Sardans, J., Peñuelas, J., and Obersteiner, M.: Global and regional phosphorus budgets in agricultural systems and their implications for phosphorus-use efficiency, Earth Syst. Sci. Data, 10, 1-18, http://doi.org/10.5194/essd-10-1-2018, 2018.

Luo, Y. Q., Su, B., Currie, W. S., Dukes, J. E., Finzi, A., Hartwig, U., Hungate, B., Mc Murtrie, R. E., Oren, R., Parton, W. J., Pataki, D. E., Rebecca Shaw, M., Zak, D. R., and Field, C. B.: Progressive

nitrogen limitation of ecosystem responses to rising atmospheric carbon dioxide, BioScience, 54(8), 731–739, https://doi.org/10.1641/0006-3568(2004)054[0731:PNLOER]2.0.CO;2, 2004.

MacBean, N., Maignan, F., Bacour, C., Lewis, P., Peylin, P., Guanter, L., Köhler, P., Gómez-Dans, J., and Disney, M.: Strong constraint on modelled global carbon uptake using solar-induced chlorophyll fluorescence data, Sci. Rep., 8, 1973, http://doi.org/10.1038/s41598-018-20024-w, 2018.

Malyshev, A. V., and Henry, H. A.: N uptake and growth responses to sub-lethal freezing in the grass Poa pratensis L, Plant Soil, 360, 175-185, http://doi.org/10.1007/s11104-012-1233-4, 2012.

Marcolla, B., Rödenbeck, C., and Cescatti, A.: Patterns and controls of inter-annual variability in the terrestrial carbon budget, Biogeosciences, 14, 3815-3829, http://doi.org/10.5194/bg-14-3815-2017, 2017.

Margalef, O., Sardans, J., Fernández-Martínez, M., Molowny-Horas, R., Janssens, I., Ciais, P., Goll, D., Richter, A., Obersteiner, M., Asensio, D., and Peñuelas, J.: Global patterns of phosphatase activity in natural soils, Sci. Rep., 7, 1-13, http://doi.org/10.1038/s41598-017-01418-8, 2017.

Mayorga, E., Seitzinger, S. P., Harrison, J. A., Dumont, E., Beusen, A. H., Bouwman, A., Fekete, B. M., Kroeze, C., and Van Drecht, G.: Global nutrient export from WaterSheds 2 (NEWS 2): model development and implementation, Environ. Modell. Softw., 25, 837-853, http://doi.org/10.1016/j.envsoft.2010.01.007, 2010.

McGill, W., and Cole, C.: Comparative aspects of cycling of organic C, N, S and P through soil organic matter, Geoderma, 26, 267-286, http://doi.org/10.1016/0016-7061(81)90024-0, 1981.

McGroddy, M. E., Daufresne, T., and Hedin, L. O.: Scaling of C: N: P stoichiometry in forests worldwide: Implications of terrestrial redfield‐type ratios, Ecology, 85, 2390-2401, http://doi.org/10.1890/03-0351, 2004.

Mekonnen, M. M., and Hoekstra, A. Y.: Global anthropogenic phosphorus loads to freshwater and associated grey water footprints and water pollution levels: A high‐resolution global study, Water Resour. Res., 54, 345-358, http://doi.org/10.1002/2017WR020448, 2018.

Melillo, J. M., Butler, S., Johnson, J., Mohan, J., Steudler, P., Lux, H., Burrows, E., Bowles, F., Smith, R., Scott, L., Vario, C., Hill, T., Burton, A., Zhou, Y., and Tang, J.: Soil warming, carbon–nitrogen interactions, and forest carbon budgets, Proc. Natl. Acad. Sci. U. S. A., 108, 9508-9512, http://doi.org/10.1073/pnas.1018189108, 2011.

Monfreda, C., Ramankutty, N., and Foley, J. A.: Farming the planet: 2. Geographic distribution of crop areas, yields, physiological types, and net primary production in the year 2000, Glob. Biogeochem. Cycle, 22, http://doi.org/10.1029/2007GB002947, 2008.

Naudts, K., Ryder, J., McGrath, M. J., Otto, J., Chen, Y., Valade, A., Bellasen, V., Berhongaray, G., Bönisch, G., Campioli, M., Ghattas, J., De Groote, T., Haverd, V., Kattge, J., MacBean, N., Maignan, F., Merilä, P., Penuelas, J., Peylin, P., Pinty, B., Pretzsch, H., Schulze, E. D., Solyga, D., Vuichard, N., Yan, Y., and Luyssaert, S.: A vertically discretised canopy description for ORCHIDEE (SVN r2290)

and the modifications to the energy, water and carbon fluxes, Geosci. Model Dev., 8, 2035–2065, https://doi.org/10.5194/gmd-8-2035-2015, 2015.

Norby, R. J., Warren, J. M., Iversen, C. M., Medlyn, B. E., and McMurtrie, R. E.: CO2 enhancement of forest productivity constrained by limited nitrogen availability, Proc. Natl. Acad. Sci. U. S. A., 107, 19368-19373, http://doi.org/10.1073/pnas.1006463107, 2010.

Osmond, C., Winter, K., and Ziegler, H.: Functional significance of different pathways of CO2 fixation in photosynthesis, in: Physiological plant ecology II, Springer, 479-547, 1982.

Peng, C., Ma, Z., Lei, X., Zhu, Q., Chen, H., Wang, W., Liu, S., Li, W., Fang, X., and Zhou, X.: A drought-induced pervasive increase in tree mortality across Canada's boreal forests, Nat. Clim. Chang., 1, 467-471, http://doi.org/10.1038/NCLIMATE1293, 2011.

Peng, J., Wang, Y. P., Houlton, B. Z., Dan, L., Pak, B., and Tang, X.: Global carbon sequestration is highly sensitive to model‐based formulations of nitrogen fixation, Glob. Biogeochem. Cycle, http://doi.org/10.1029/2019GB006296, 2019.

Peng, S., Ciais, P., Maignan, F., Li, W., Chang, J., Wang, T., and Yue, C.: Sensitivity of land use change emission estimates to historical land use and land cover mapping, Glob. Biogeochem. Cycle, 31, 626-643, http://doi.org/10.1002/2015GB005360, 2017.

Penuelas, J., Poulter, B., Sardans, J., Ciais, P., Van Der Velde, M., Bopp, L., Boucher, O., Godderis, Y., Hinsinger, P., Llusia, J., Nardin, E., Vicca, S., Obersteiner, M., and Janssens, I. A.: Human-induced nitrogen–phosphorus imbalances alter natural and managed ecosystems across the globe, Nat. Commun., 4, 1-10, http://doi.org/10.1038/ncomms3934, 2013.

Piao, S., Luyssaert, S., Ciais, P., Janssens, I. A., Chen, A., Cao, C., Fang, J., Friedlingstein, P., Luo, Y., and Wang, S.: Forest annual carbon cost: A global‐scale analysis of autotrophic respiration, Ecology, 91, 652-661, http://doi.org/10.1890/08-2176.1, 2010.

Piao, S., Sitch, S., Ciais, P., Friedlingstein, P., Peylin, P., Wang, X., Ahlström, A., Anav, A., Canadell, J. G., Cong, N., Huntingford, C., Jung, M., Levis, S., Levy, P. E., Li, J., Lin, X., Lomas, M. R., Lu, M., Luo, Y., Ma, Y., Myneni, R. B., Poulter, B., Sun, Z., Wang, T., Viovy, N., Zaehle, S., and Zeng, N.: Evaluation of terrestrial carbon cycle models for their response to climate variability and to CO2 trends, Global Change Biol., 19, 2117– 2132, http://doi.org/10.1111/gcb.12187, 2013.

Poulter, B., Ciais, P., Hodson, E., Lischke, H., Maignan, F., Plummer, S., and Zimmermann, N.: Plant functional type mapping for earth system models, Geosci. Model Dev., 4, 993-1010, http://doi.org/10.5194/gmd-4-993-2011, 2011.

Poulter, B., MacBean, N., Hartley, A., Khlystova, I., Arino, O., Betts, R., Bontemps, S., Boettcher, M., Brockmann, C., Defourny, P., Hage- mann, S., Herold, M., Kirches, G., Lamarche, C., Lederer, D., Ottlé, C., Peters, M., and Peylin, P.: Plant functional type classification for earth system models: Results from the European Space Agency's Land Cover Climate Change Initiative, Geoscientific Model Develop- ment, 8, 2315–2328, https://doi.org/10.5194/gmd-8-2315-2015, 2015.

Prentice, I. C., Liang, X., Medlyn, B. E., and Wang, Y.: Reliable, robust and realistic: the three R's of next-generation land-surface modelling, Atmos. Chem. Phys., http://doi.org/10.5194/acp-15-5987-2015, 2015.

Pugh, T. A., Lindeskog, M., Smith, B., Poulter, B., Arneth, A., Haverd, V., and Calle, L.: Role of forest regrowth in global carbon sink dynamics, Proc. Natl. Acad. Sci. U. S. A., 116, 4382-4387, http://doi.org/10.1073/pnas.1810512116, 2019.

Recous, S., Robin, D., Darwis, D., and Mary, B.: Soil inorganic N availability: effect on maize residue decomposition, Soil Biol. Biochem., 27, 1529-1538, http://doi.org/10.1016/0038-0717(95)00096-W, 1995.

Reed, S. C., Townsend, A. R., Davidson, E. A., and Cleveland, C. C.: Stoichiometric patterns in foliar nutrient resorption across multiple scales, New Phytol., 196, 173-180, http://doi.org/10.1111/j.1469-8137.2012.04249.x, 2012.

Reich, P. B., and Oleksyn, J.: Global patterns of plant leaf N and P in relation to temperature and latitude, Proc. Natl. Acad. Sci. U. S. A., 101, 11001-11006, http://doi.org/10.1073/pnas.0403588101, 2004.

Rennenberg, H., Dannenmann, M., Gessler, A., Kreuzwieser, J., Simon, J., and Papen, H.: Nitrogen balance in forest soils: nutritional limitation of plants under climate change stresses, Plant Biol., 11, 4-23, http://doi.org/10.1111/j.1438-8677.2009.00241.x, 2009.

Rödenbeck, C., Houweling, S., Gloor, M., and Heimann, M.: CO2 flux history 1982-2001 inferred from atmospheric data using a global inversion of atmospheric transport, Atmos. Chem. Phys., 3, 1919-1964, 2003.

Running, S. W., Nemani, R. R., Heinsch, F. A., Zhao, M., Reeves, M., and Hashimoto, H.: A continuous satellite-derived measure of global terrestrial primary production, BioScience, 54, 547-560, http://doi.org/10.1641/0006-3568(2004)054[0547:ACSMOG]2.0.CO;2, 2004.

Ryu, Y., Verfaillie, J., Macfarlane, C., Kobayashi, H., Sonnentag, O., Vargas, R., Ma, S., and Baldocchi, D. D.: Continuous observation of tree leaf area index at ecosystem scale using upward-pointing digital cameras, Remote Sens. Environ., 126, 116-125, http://doi.org/10.1016/j.rse.2012.08.027, 2012.

Saatchi, S. S., Harris, N. L., Brown, S., Lefsky, M., Mitchard, E. T., Salas, W., Zutta, B. R., Buermann, W., Lewis, S. L., Hagen, S., Petrova, S., White, L., Silman, M., Morel, A.: Benchmark map of forest carbon stocks in tropical regions across three continents, Proc. Natl. Acad. Sci. U. S. A., 108, 9899-9904, http://doi.org/10.1073/pnas.1019576108, 2011.

Santoro, M., Eriksson, L. E., and Fransson, J. E.: Reviewing ALOS PALSAR backscatter observations for stem volume retrieval in Swedish forest, Remote Sens., 7, 4290-4317, http://doi.org/10.3390/rs70404290, 2015.

Shane, M. W., McCully, M. E., Canny, M. J., Pate, J. S., Ngo, H., Mathesius, U., Cawthray, G. R., and Lambers, H.: Summer dormancy and winter growth: root survival strategy in a perennial monocotyledon, New Phytol., 183, 1085-1096, http://doi.org/10.1111/j.1469-8137.2009.02875.x, 2009.

Sigurdsson, B. D., Medhurst, J. L., Wallin, G., Eggertsson, O., and Linder, S.: Growth of mature boreal Norway spruce was not affected by elevated [CO2] and/or air temperature unless nutrient availability was improved, Tree Physiol., 33, 1192-1205, http://doi.org/10.1093/treephys/tpt043, 2013.

Sitch, S., Friedlingstein, P., Gruber, N., Jones, S. D., Murray- Tortarolo, G., Ahlström, A., Doney, S. C., Graven, H., Heinze, C., Huntingford, C., Levis, S., Levy, P. E., Lomas, M., Poul- ter, B., Viovy, N., Zaehle, S., Zeng, N., Arneth, A., Bonan, G., Bopp, L., Canadell, J. G., Chevallier, F., Ciais, P., Ellis, R., Gloor, M., Peylin, P., Piao, S. L., Le Quéré, C., Smith, B., Zhu, Z., and Myneni, R.: Recent trends and drivers of regional sources and sinks of carbon dioxide, Biogeosciences, 12, 653– 679, http://doi.org/10.5194/bg-12-653-2015, 2015.

Smith, W. K., Reed, S. C., Cleveland, C. C., Ballantyne, A. P., Anderegg, W. R., Wieder, W. R., Liu, Y. Y., and Running, S. W.: Large divergence of satellite and Earth system model estimates of global terrestrial CO2 fertilization, Nat. Clim. Chang., 6, 306-310, http://doi.org/10.1038/NCLIMATE2879, 2016.

Soussana, J.-F., and Lemaire, G.: Coupling carbon and nitrogen cycles for environmentally sustainable intensification of grasslands and crop-livestock systems, Agric. Ecosyst. Environ., 190, 9-17, http://doi.org/10.1016/j.agee.2013.10.012, 2014.

Stephens, B. B., Gurney, K. R., Tans, P. P., Sweeney, C., Pe- ters, W., Bruhwiler, L., Ciais, P., Ramonet, M., Bousquet, P., Nakazawa, T., Aoki, S., Machida, T., Inoue, G., Vinnichenko, N., Lloyd, J., Jordan, A., Heimann, M., Shibistova, O., Langen- felds, R. L., Steele, L. P., Francey, R. J., and Denning, A. S.: Weak northern and strong tropical land carbon uptake from ver- tical profiles of atmospheric CO2, Science, 316, 1732–1735, , http://doi.org/10.1126/science.1137004, 2007.

Sterner, R. W., and Elser, J. J.: Ecological stoichiometry: the biology of elements from molecules to the biosphere, Princeton university press, 2002.

Stocker, B. D., Zscheischler, J., Keenan, T. F., Prentice, I. C., Seneviratne, S. I., and Peñuelas, J.: Drought impacts on terrestrial primary production underestimated by satellite monitoring, Nat. Geosci., 12, 264-270, http://doi.org/10.1038/s41561-019-0318-6, 2019.

Sullivan, B. W., Smith, W. K., Townsend, A. R., Nasto, M. K., Reed, S. C., Chazdon, R. L., and Cleveland, C. C.: Spatially robust estimates of biological nitrogen (N) fixation imply substantial human alteration of the tropical N cycle, Proc. Natl. Acad. Sci. U. S. A., 111, 8101-8106, http://doi.org/10.1073/pnas.1320646111, 2014.

Sulman, B. N., Brzostek, E. R., Medici, C., Shevliakova, E., Menge, D. N., and Phillips, R. P.: Feedbacks between plant N demand and rhizosphere priming depend on type of mycorrhizal association, Ecol. Lett., 20, 1043-1053, http://doi.org/10.1111/ele.12802, 2017.

Sun, Y., Peng, S., Goll, D. S., Ciais, P., Guenet, B., Guimberteau, M., Hinsinger, P., Janssens, I. A., Peñuelas, J., Piao, S., Poulter, B., Violette, A., Yang, X., Yin, Y., and Zeng, H.: Diagnosing phosphorus limitations in natural terrestrial ecosystems in carbon cycle models, Earths Future, 5, 730-749, http://doi.org/10.1002/2016EF000472, 2017.

Sun, Y., Goll, D. S., Ciais, P., Peng, S., Margalef, O., Asensio, D., Sardans, J., and Peñuelas, J.: Spatial pattern and environmental drivers of acid phosphatase activity in Europe, Front. Big Data, http://doi.org/10.3389/fdata.2019.00051, 2020.

Sun, Z., Wang, X., Zhang, X., Tani, H., Guo, E., Yin, S., and Zhang, T.: Evaluating and comparing remote sensing terrestrial GPP models for their response to climate variability and CO2 trends, Sci. Total Environ., 668, 696-713, http://doi.org/10.1016/j.scitotenv.2019.03.025, 2019.

Terrer, C., Jackson, R.B., Prentice, I.C., Keenan, T.F., Kaiser, C., Vicca, S., Fisher, J.B., Reich, P.B., Stocker, B.D., Hungate, B.A., Peñuelas, J., McCallum, I., Soudzilovskaia, N.A., Cernusak, L.A., Talhelm, A.F., van Sundert, K., Piao, S., Newton, P.C.D., Hovenden, M.J., Blumenthal, D.M., Liu, Y.Y., Müller, C., Winter, K., Field, C.B., Viechtbauer, W., van Lissa, C.J., Hoosbeek, M.R., Watanabe, M., Koike, T., Leshyk, V.O., Polley, H.W., and Franklin, O.: Nitrogen and phosphorus constrain the CO2 fertilization of global plant biomass, Nat. Clim. Chang., 9, 684-689, http://doi.org/10.1038/s41558-019-0545-2, 2019.

Thornton, P. E., Lamarque, J. F., Rosenbloom, N. A., and Mahowald, N. M.: Influence of carbon‐nitrogen cycle coupling on land model response to CO2 fertilization and climate variability, Glob. Biogeochem. Cycle, 21, http://doi.org/10.1029/2006GB002868, 2007.

Thum, T., Caldararu, S., Engel, J., Kern, M., Pallandt, M., Schnur, R., Yu, L., and Zaehle, S.: A new terrestrial biosphere model with coupled carbon, nitrogen, and phosphorus cycles (QUINCY v1. 0; revision 1772), Geosci. Model Dev., 12, 4781-4802, http://doi.org/10.5194/gmd-12-4781-2019, 2019.

Tipping, E., Somerville, C. J., and Luster, J.: The C: N: P: S stoichiometry of soil organic matter, Biogeochemistry, 130, 117-131, http://doi.org/10.1007/s10533-016-0247-z, 2016.

Tum, M., Zeidler, J., Günther, K. P., and Esch, T.: Global NPP and straw bioenergy trends for 2000–2014, Biomass Bioenerg., 90, 230-236, http://doi.org/10.1016/j.biombioe.2016.03.040, 2016.

Turner, D. P., Ritts, W. D., Cohen, W. B., Gower, S. T., Running, S. W., Zhao, M., Costa, M. H., Kirschbaum, A. A., Ham, J. M., Saleska, S. R., and Ahl, D.: Evaluation of MODIS NPP and GPP products across multiple biomes, Remote Sens. Environ., 102, 282-292, http://doi.org/10.1016/j.rse.2006.02.017, 2006.

van der Laan-Luijkx IT, van der Velde IR, van der Veen E, Tsuruta A, Stanislawska K, Babenhauserheide A, Zhang HF, Liu Y, He W, Chen H, Masarie KA, Krol MC, and Peters W: The CarbonTracker Data Assimilation Shell (CTDAS) v1. 0: implementation and global carbon balance 2001-2015, Geosci. Model Dev., 10, 2785-2800, http://doi.org/10.5194/gmd-10-2785-2017, 2017.

Vergutz, L., Manzoni, S., Porporato, A., Novais, R. F., and Jackson, R. B.: Global resorption efficiencies and concentrations of carbon and nutrients in leaves of terrestrial plants, Ecol. Monogr., 82, 205-220, http://doi.org/10.1890/11-0416.1, 2012.

Vitousek, P. M., Menge, D. N., Reed, S. C., and Cleveland, C. C.: Biological nitrogen fixation: rates, patterns and ecological controls in terrestrial ecosystems, Philos. Trans. R. Soc. B-Biol. Sci., 368, 20130119, http://doi.org/10.1098/rstb.2013.0119, 2013.

Vuichard, N., Messina, P., Luyssaert, S., Guenet, B., Zaehle, S., Ghattas, J., Bastrikov, V., and Peylin, P.: Accounting for carbon and nitrogen interactions in the global terrestrial ecosystem model ORCHIDEE (trunk version, rev 4999): multi-scale evaluation of gross primary production, Geosci. Model Dev., 12, 4751-4779, http://doi.org/10.5194/gmd-12-4751-2019, 2019.

Walker, A. P., De Kauwe, M. G., Medlyn, B. E., Zaehle, S., Iversen, C. M., Asao, S., Guenet, B., Harper, A., Hickler, T., Hungate, B. A., Jain, A. K., Luo, Y., Lu, X., Lu, M., Luus, K., Megonigal, J. P., Oren, R., Ryan, E., Shu, S., Talhelm, A., Wang, Y., Warren, J. M., Werner, C., Xia, J., Yang, B., Zak, D. R., and Norby, R. J.: Decadal biomass increment in early secondary succession woody ecosystems is increased by CO2 enrichment, Nat. Commun., 10, 1-13, http://doi.org/10.1038/s41467-019-08348-1, 2019.

Wanek, W., Zezula, D., Wasner, D., Mooshammer, M., and Prommer, J.: A novel isotope pool dilution approach to quantify gross rates of key abiotic and biological processes in the soil phosphorus cycle, Biogeosciences, 16, 3047-3068, http://doi.org/10.5194/bg-16-3047-2019, 2019.

Wang, C., Han, G., Jia, Y., Feng, X., Guo, P., and Tian, X.: Response of litter decomposition and related soil enzyme activities to different forms of nitrogen fertilization in a subtropical forest, Ecol. Res., 26, 505-513, http://doi.org/10.1007/s11284-011-0805-8, 2011.

Wang, R., Goll, D., Balkanski, Y., Hauglustaine, D., Boucher, O., Ciais, P., Janssens, I., Penuelas, J., Guenet, B., Sardans, J., Bopp, L., Vuichard, N., Zhou, F., Li, B., Piao, S., Peng, S., Huang, Y., and Tao, S.: Global forest carbon uptake due to nitrogen and phosphorus deposition from 1850 to 2100, Glob. Change Biol., 23, 4854-4872, http://doi.org/10.1111/gcb.13766, 2017.

Wang, Y., Law, R., and Pak, B.: A global model of carbon, nitrogen and phosphorus cycles for the terrestrial biosphere, Biogeosciences, 7, http://doi.org/10.5194/bg-7-2261-2010, 2010.

Wang, Y., Ciais, P., Goll, D. S., Huang, Y., Luo, Y., Wang, Y.-P., Bloom, A. A., Broquet, G., Hartmann, J., Peng, S., Penuelas, J., Piao, S., Sardans, J., Stocker, B., Wang, R., Zaehle, S., and Zechmeister-Boltenstern, S.: GOLUM-CNP v1. 0: a data-driven modeling of carbon, nitrogen and phosphorus cycles in major terrestrial biomes, Geosci. Model Dev, http://doi.org/10.5194/gmd-11-3903-2018, 2018.

Wang, Y. P., Houlton, B., and Field, C.: A model of biogeochemical cycles of carbon, nitrogen, and phosphorus including symbiotic nitrogen fixation and phosphatase production, Glob. Biogeochem. Cycle, 21, http://doi.org/10.1029/2006GB002797, 2007.

Wang, Y. P., and Houlton, B. Z.: Nitrogen constraints on terrestrial carbon uptake: Implications for the global carbon‐climate feedback, Geophys. Res. Lett., 36, http://doi.org/10.1029/2009GL041009, 2009.

Warren, J. M., Hanson, P. J., Iversen, C. M., Kumar, J., Walker, A. P., and Wullschleger, S. D.: Root structural and functional dynamics in terrestrial biosphere models–evaluation and recommendations, New Phytol., 205, 59-78, http://doi.org/10.1111/nph.13034, 2015.

Wieder, W. R., Cleveland, C. C., Smith, W. K., and Todd-Brown, K.: Future productivity and carbon storage limited by terrestrial nutrient availability, Nat. Geosci., 8, 441-444, http://doi.org/10.1038/NGEO2413, 2015.

Williams, M., Richardson, A. D., Reichstein, M., Stoy, P. C., Peylin, P., Verbeeck, H., Carvalhais, N., Jung, M., Hollinger, D. Y., Kattge, J., Leuning, R., Luo, Y., Tomelleri, E., Trudinger, C. M., and Wang, Y. P.: Improving land surface models with FLUXNET data, Biogeosciences, http://doi.org/10.5194/bg-6-1341-2009, 2009.

Wißkirchen, K., Tum, M., Günther, K., Niklaus, M., Eisfelder, C., and Knorr, W.: Quantifying the carbon uptake by vegetation for Europe on a 1km 2 resolution using a remote sensing driven vegetation model, Geosci. Model Dev., 6, http://doi.org/10.5194/gmd-6-1623-2013, 2013.

Wright, S. J.: Plant responses to nutrient addition experiments conducted in tropical forests, Ecol. Monogr., 89, e01382, http://doi.org/10.1002/ecm.1382, 2019.

Xu, X., Jain, A. K., and Calvin, K. V.: Quantifying the biophysical and socioeconomic drivers of changes in forest and agricultural land in South and Southeast Asia, Glob. Change Biol., 25, 2137-2151, http://doi.org/10.1111/gcb.14611, 2019.

Yang, X., Wittig, V., Jain, A. K., and Post, W.: Integration of nitrogen cycle dynamics into the Integrated Science Assessment Model for the study of terrestrial ecosystem responses to global change, Glob. Biogeochem. Cycle, 23, http://doi.org/10.1029/2009GB003474, 2009.

Yang, X., Thornton, P., Ricciuto, D., and Post, W.: The role of phosphorus dynamics in tropical forests--a modeling study using CLM-CNP, Biogeosciences, 11, http://doi.org/10.5194/bg-11-1667-2014, 2014.

Yuan, Z., and Chen, H. Y.: Decoupling of nitrogen and phosphorus in terrestrial plants associated with global changes, Nat. Clim. Chang., 5, 465-469, http://doi.org/10.1038/NCLIMATE2549, 2015.

Zaehle, S., and Friend, A.: Carbon and nitrogen cycle dynamics in the O‐CN land surface model: 1. Model description, site‐scale evaluation, and sensitivity to parameter estimates, Glob. Biogeochem. Cycle, 24, http://doi.org/10.1029/2009GB003521, 2010.

Zaehle, S., Jones, C. D., Houlton, B., Lamarque, J.-F., and Robertson, E.: Nitrogen availability reduces CMIP5 projections of twenty-first-century land carbon uptake, J. Clim., 28, 2494-2511, http://doi.org/10.1175/JCLI-D-13-00776.1, 2015.

Zaehle, S., Medlyn, B. E., De Kauwe, M. G., Walker, A. P., Dietze, M. C., Hickler, T., Luo, Y., Wang, Y.-P., El-Masri, B., Thornton, P., Jain, A., Wang, S., Warlind, D., Weng, E., Parton, W., Iversen, C. M., Gallet-Budynek, A., McCarthy, H., Finzi, A., Hanson, P. J., Prentice, I. C., Oren, R., and Norby, R. J.: Evaluation of 11 ter- restrial carbon–nitrogen cycle models against observations from two temperate Free-Air CO2 Enrichment studies, New Phytol., 202, 803–822, http://doi.org/10.1111/nph.12697, 2014.

Zechmeister-Boltenstern, S., Keiblinger, K. M., Mooshammer, M., Peñuelas, J., Richter, A., Sardans, J., and Wanek, W.: The application of ecological stoichiometry to plant–microbial–soil organic matter transformations, Ecol. Monogr., 85, 133-155, http://doi.org/10.1890/14-0777.1, 2015.

Zhang, B., Tian, H., Lu, C. C., Dangal, S. R., Yang, J., and Pan, S.: Global manure nitrogen production and application in cropland during 1860–2014: a 5 arcmin gridded global dataset for Earth system modeling, Earth Syst. Sci. Data, 9, 667, http://doi.org/10.5194/essd-9-667-2017, 2017.

Zhang, H., Goll, D. S., Manzoni, S., Ciais, P., Guenet, B., and Huang, Y.: Modeling the effects of litter stoichiometry and soil mineral N availability on soil organic matter formation using CENTURY-CUE (v1. 0), Geosci. Model Dev., http://doi.org/10.5194/gmd-11-4779-2018, 2018.

Zhang, H., Goll, D. S., Wang, Y. P., Ciais, P., Wieder, W. R., Abramoff, R., Huang, Y., Guenet, B., Prescher, A. K., Viscarra Rossel, R. A., Barré, P., Chenu, C., Zhou, G., and Tang, X.: Microbial dynamics and soil physicochemical properties explain large‐scale variations in soil organic carbon, Glob. Change Biol., http://doi.org/10.1111/gcb.14994, 2020.

Zhang, X., Davidson, E. A., Mauzerall, D. L., Searchinger, T. D., Dumas, P., and Shen, Y.: Managing nitrogen for sustainable development, Nature, 528, 51-59, http://doi.org/10.1038/nature15743, 2015.

Zhao, M., Heinsch, F. A., Nemani, R. R., and Running, S. W.: Improvements of the MODIS terrestrial gross and net primary production global data set, Remote Sens. Environ., 95, 164-176, http://doi.org/10.1016/j.rse.2004.12.011, 2005.

Zhu, Z., Bi, J., Pan, Y., Ganguly, S., Anav, A., Xu, L., Samanta, A., Piao, S., Nemani, R. R., and Myneni, R. B.: Global data sets of vegetation leaf area index (LAI) 3g and fraction of photosynthetically active radiation (FPAR) 3g derived from global inventory modeling and mapping studies (GIMMS) normalized difference vegetation index (NDVI3g) for the period 1981 to 2011, Remote Sens. , 5, 927-948, http://doi.org/10.3390/rs5020927 2013.

Zhu, P., Zhuang, Q., Ciais, P., Welp, L., Li, W., and Xin, Q.: Elevated atmospheric CO2 negatively impacts photosynthesis through radiative forcing and physiology‐mediated climate feedback, Geophys. Res. Lett., 44, 1956-1963, http://doi.org/10.1002/2016GL071733, 2017.

Zobler, L.: A world soil file global climate modeling, 32, 1986.

335 **Table 1 Main information on datasets used for global evaluation of ORCHIDEE-CNP.**

Dataset	Variable	Resolution	Period	Uncertainties	References
MODIS	GPP, NPP, CUE	1km	2000-2015	Bias against local measurements for GPP and NPP	Running et al., 2004; Zhao et al., 2005; Turner et al., 2006;
MTE	GPP, WUE	0.5°	1982-2011	25 ensemble trees for GPP and ET respectively	Jung et al., 2009; Jung et al., 2011
BESS	GPP	0.5°	2001-2015	Bias against local measurements	Ryu et al., 2011; Jiang and Ryu, 2016
BETHY	NPP	0.008°	2000-2009	-	Tum et al., 2016; Wißkirchen et al., 2013
GIMMS	NPP	0.5°	1982-2015	Using different climate inputs	Smith et al., 2016
Trendy v6	NBP	0.5°	1959-2016	1-sigma standard deviation	Sitch et al., 2013
JENA_inversion	NBP	1°	1985-2016	-	Rödenbeck et al., 2003
CAMS inversion	NBP	1.875°x3.75°	1979-2016	-	Chevallier et al., 2005
Ctracker inversion	NBP	1°	2001-2016	-	van der Laan-Luijkx et al., 2017
Peng-BNF	BNF	biome	2001-2009	-	Peng et al., 2019
Sullivan-BNF	BNF	biome	1999, 2009	-	Sullivian et al., 2014
Mayorga	N & P leaching	polygon	2000	-	Mayorga et al. 2010
Helfenstein	K_m	Soil order	-	-	Helfenstein et al., 2018
Sun	Pasae activity	10km	-	-	Sun et al., 2020
GOLUM-CNP	C, N and P fluxes, N and P openness and turnover rate, PUE, NUE	0.25°	2001-2010	-	Wang et al., 2018
Global SeaWiFS Level-3 data and MTE-GPP	LUE	0.01°	1997-2006	-	Gobron et al., 2006a, b
Butler	Leaf N: P ratio	1km		100 estimates by Bayes method	Butler et al., 2017
Site leaf measurements	Leaf N:P ratio	site	-	-	Kerkhoff et al., 2005; McGroddy et al., 2004; Reich and Oleksyn, 2004
Tipping	SOM C, N and P	site	-	-	Tipping et al., 2016
Site measurements of NUE and PUE	NUE and PUE	site	-	-	Gill and Finzi, 2016

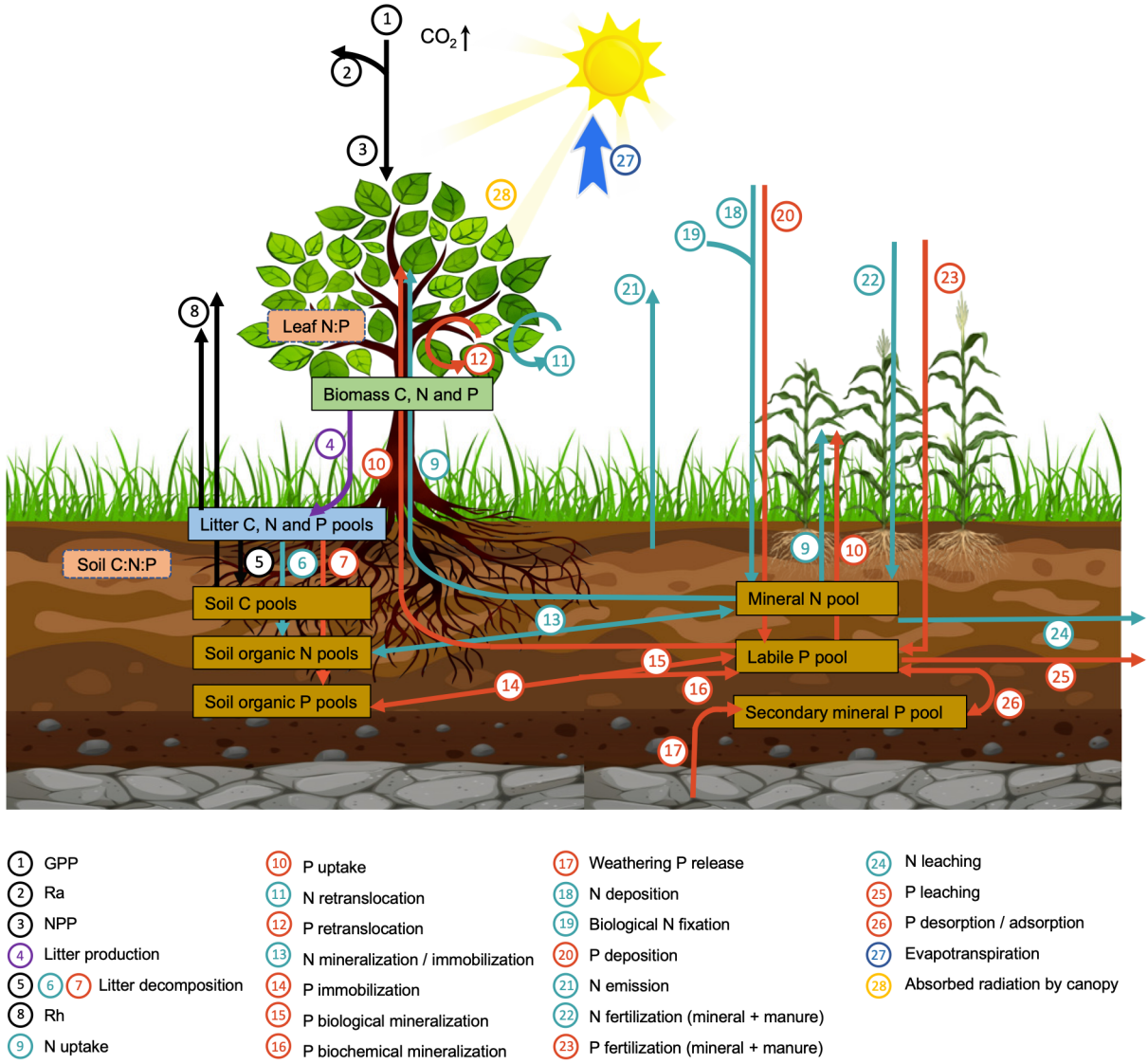

Figure 1: Schematic of C, N and P cycles considered in ORCHIDEE-CNP.

340

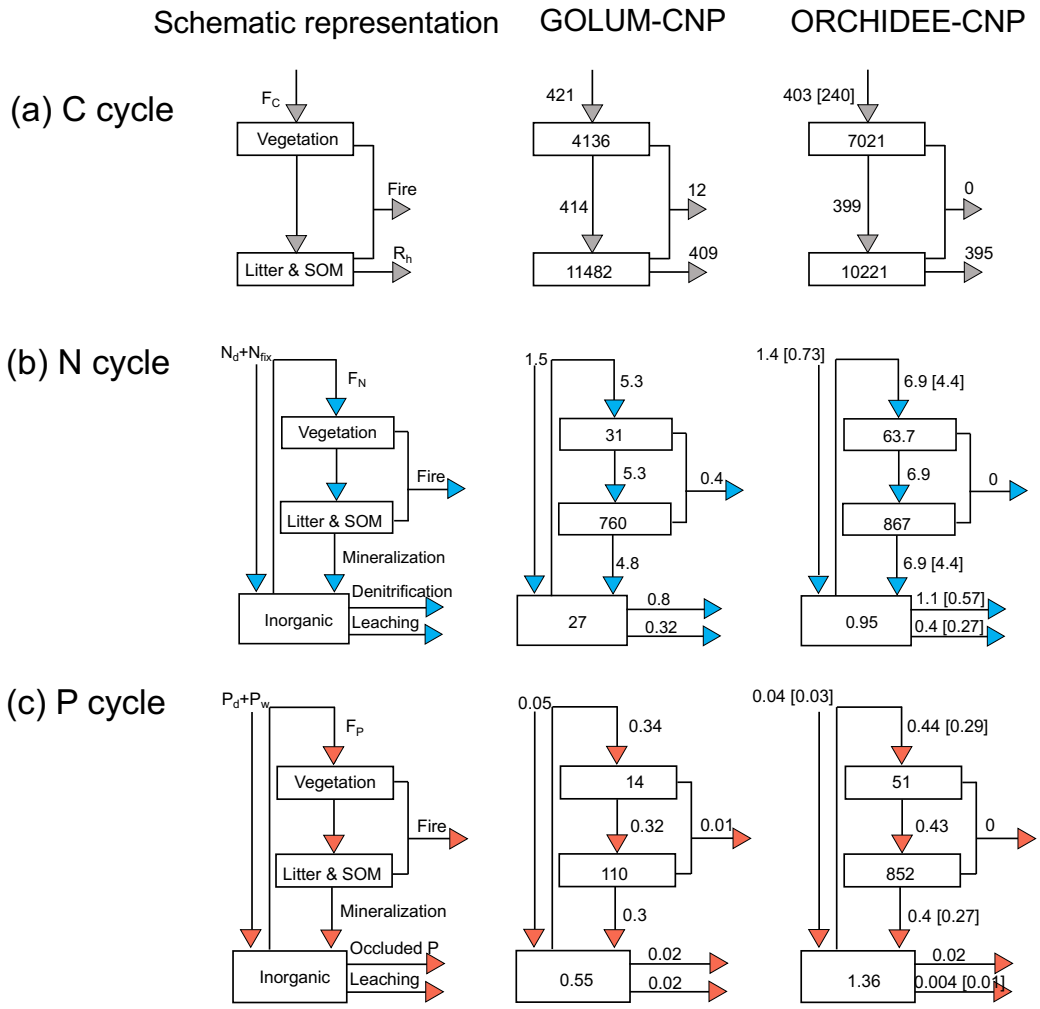

Figure 2: Flow chart of mean flows and storages per area of C, N and P (gC/gN/gP m^{-2} yr^{-1}) in natural biomes for GOLUM-CNP and ORCHIDEE-CNP. GOLUM-CNP stands for Global Observation-based Land-ecosystems Utilization Model of Carbon, Nitrogen and Phosphorus (GOLUM-CNP) v1.0, which is a data-driven model of steady-state C, N and P cycles for present day (2001-2016) conditions. C, N and P losses via fire in ORCHIDEE-CNP are ignored. Numbers in square brackets indicate the standard deviations for accounting the spatial spread of C, N and P fluxes.

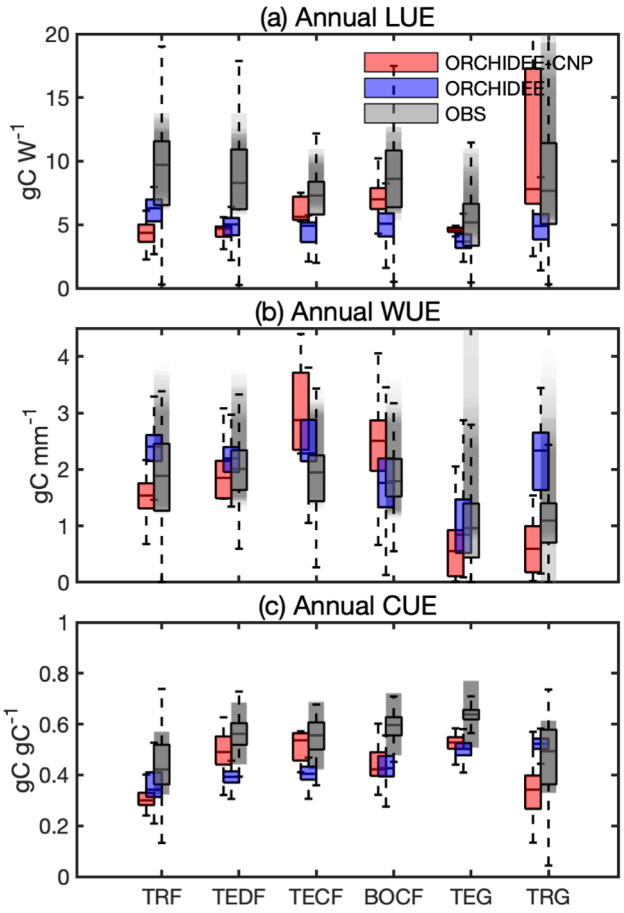

Figure 3: Comparison of annual use efficiencies of light (LUE), water (WUE) and carbon (CUE) between ORCHIDEE-CNP, ORCHIDEE and satellite-based estimations for 6 biomes: tropical rainforest (TRF), temperate deciduous forest (TEDF), temperate conifer forest (TECF), boreal conifer forest (BOCF), temperate grass (TEG) and tropical grass (TRG). The whiskers indicate the interquartile (box) and 95 % confidence intervals (dashed lines). Grey boxes indicate the satellite-based estimations (referenced). The grey shaded areas indicate the uncertainties of resource use efficiencies given by referenced estimations, which involves uncertainties for multi-estimations and spatial variability for each estimation.

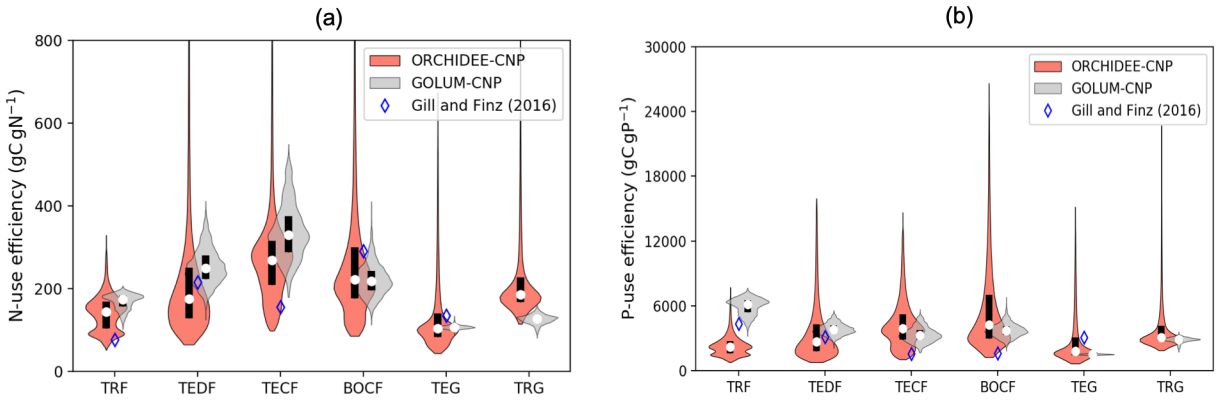

395 **Figure 4: Violin plots of nitrogen use efficiency (NUE; a) and phosphorus use efficiency (PUE; b) by ORCHIDEE-CNP, GOLUM-CNP and observations (Gill and Finzi, 2018) for 6 biomes: tropical rainforest (TRF), temperate deciduous forest (TEDF), temperate conifer forest (TECF), boreal conifer forest (BOCF), temperate grass (TEG) and tropical grass (TRG). Open circles are medians of all grid cells within each biome, with balloons representing the probability density distribution of each value. Black whiskers indicate the interquartile.**

400

405

410

415

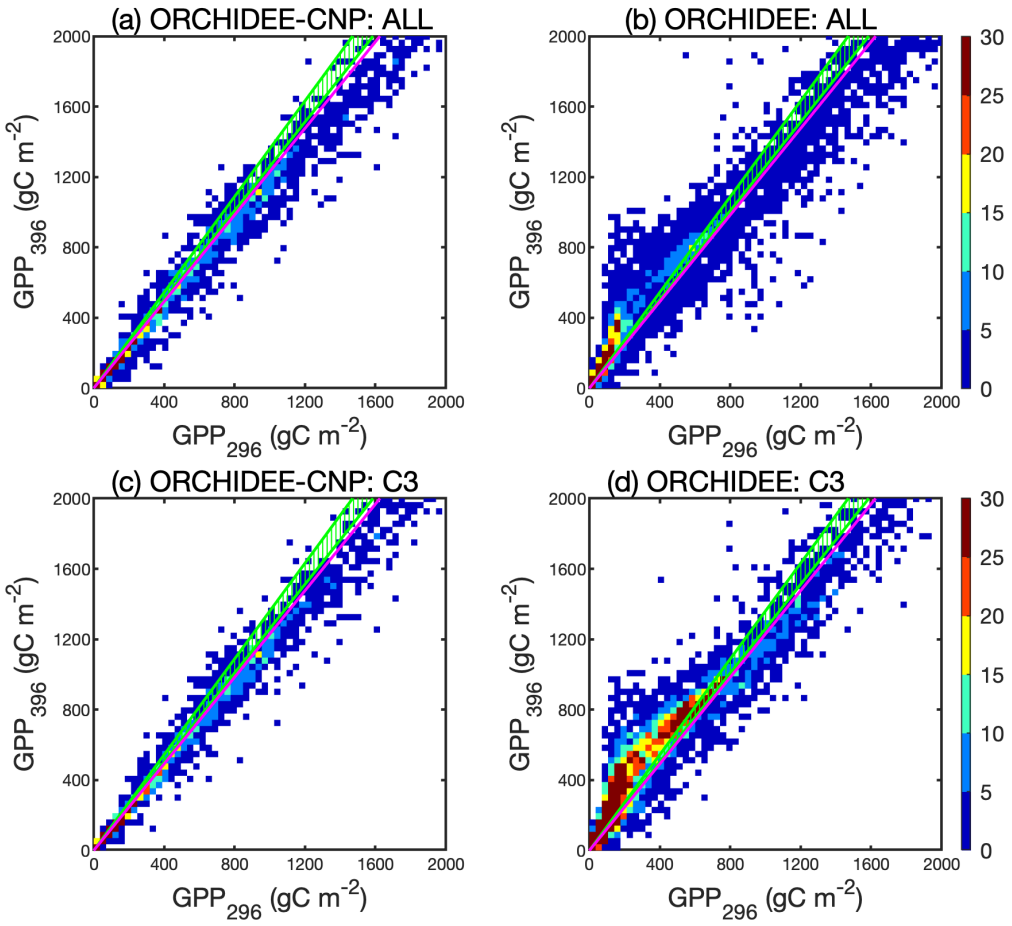

Figure 5: Comparisons between pre-industrial GPP with atmospheric CO_2 concentration of 296 ppm (GPP_{296}) and current GPP with atmospheric CO_2 concentration of 396 ppm (GPP_{396}) for all natural plants (a, b) and natural C3 plants (c, d) by ORCHIDEE-CNP (a, c) and ORCHIDEE (b, d). The color scale shows the point density. Different point density and patch size for ORCHIDEE and ORCHIDEE-CNP are due to the different spatial resolution (2^o x 2^o for ORCHIDEE-CNP and 0.5^o x 0.5^o for ORCHIDEE). The ratio between GPP_{396} and GPP_{296} indicates the CO_2 fertilization effects (E_{CO2}). Green dashed areas indicate the observed E_{CO2} from Campbell et al (2017)'s COS records. Pink lines indicate the observed E_{CO2} from Ehlers et al (2015)'s.

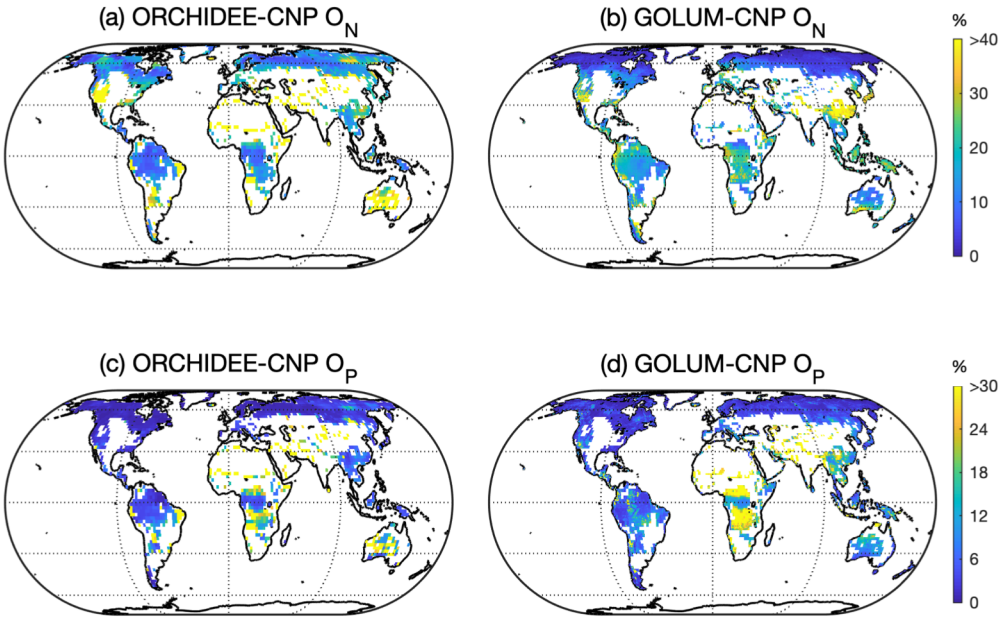

Figure 6: Global pattern of N (O_N, a-b) and P openness and (O_P, c-d) simulated by ORCHIDEE-CNP (a, c) and GOLUM-CNP (b, d). Pixels with managed lands >50% in ORCHIDEE-CNP were masked. Same area was masked from the pattern of O_N and O_P for GOLUM-CNP.

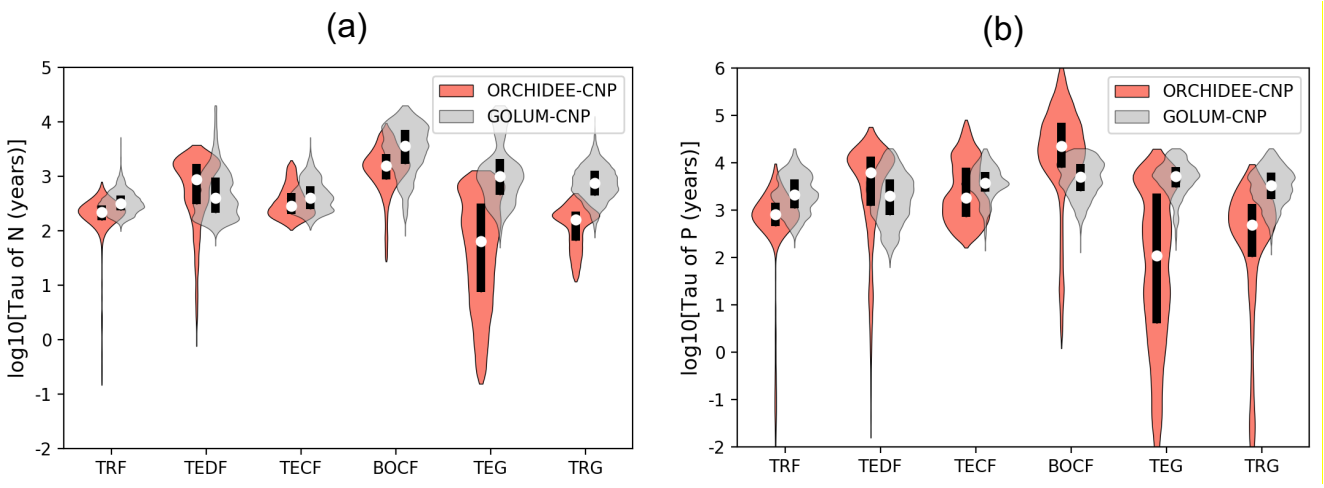

460 **Figure 7: Violin plots of residence time (c, d) of N and P cycles for 6 biomes: tropical rainforest (TRF), temperate deciduous forest (TEDF), temperate coniferous forest (TECF), boreal coniferous forest (BOCF), temperate grass (TEG) and tropical grass (TRG). Open circles are medians of all grid cells within each biome, with balloons representing the probability density distribution of each value. Black whiskers indicate the interquartile.**

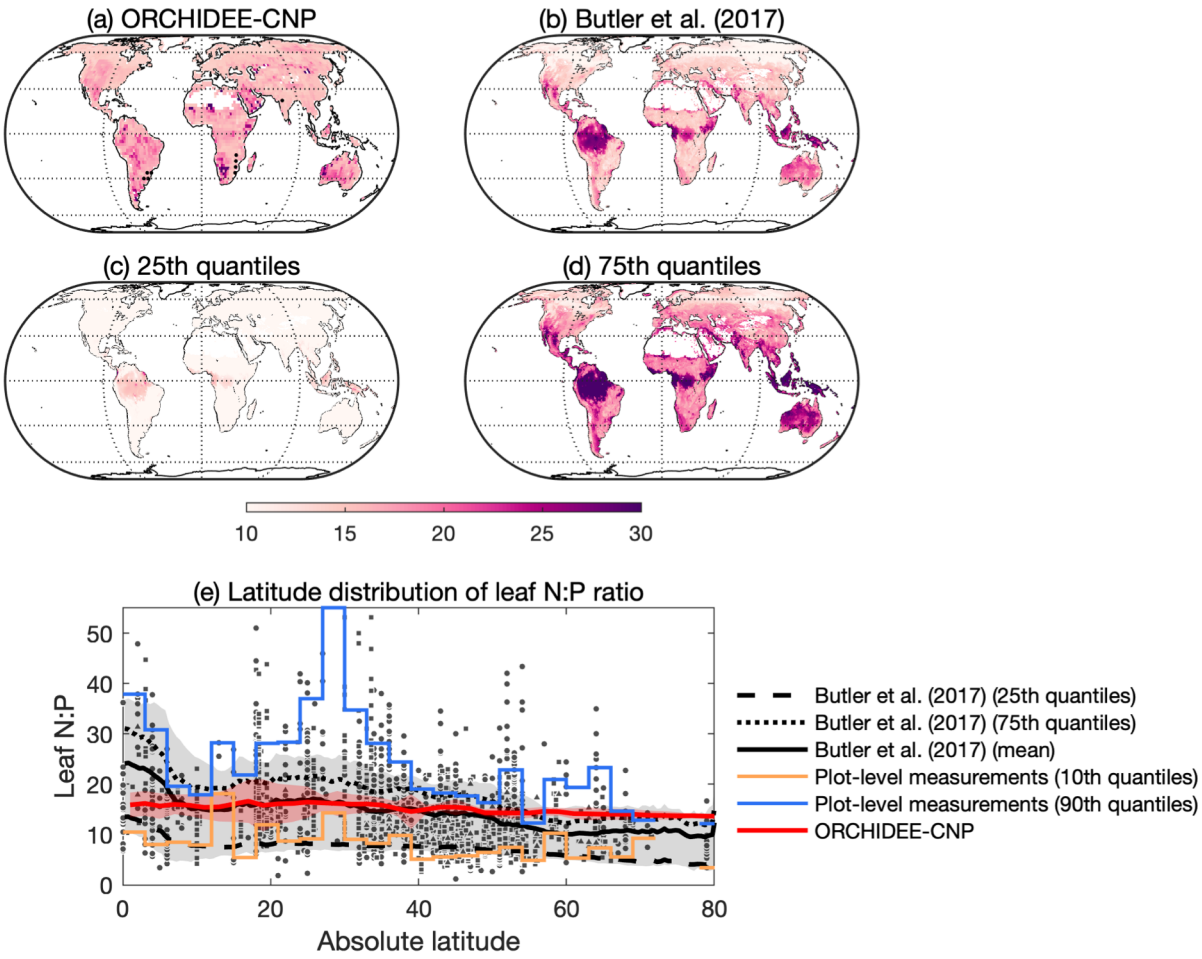

Figure 8: Comparisons of leaf N:P ratio between ORCHIDEE-CNP, data-driven estimates and observations. (a) is the global pattern of mean leaf N:P ratio over 2001-2016 for ORCHIDEE, (b) is for mean leaf N:P in Butler et al. (2017). (c) and (d) are 25% and 75% percentile of leaf N:P ratio by Butler et al. (2017), respectively. Dots in (a) indicate the area with leaf N:P ratio of ORCHIDEE-CNP falling into 25%~75% percentiles of Butler et al., (2017)'s estimation. (d) is the latitude distributions of leaf N:P ratio for ORCHIDEE-CNP, Butler et al (2017)'s estimation and site measurements. Red shared area indicates the uncertainty from latitudinal spreads of leaf N:P ratio for ORCHIDEE-CNP. Grey shaded area indicates the uncertainty from both the estimations and latitudinal spreads for Butler et al., (2017). Blue and yellow lines indicate the 10% and 90% percentiles of measured leaf N:P ratios in each bins of 3o latitude, respectively.

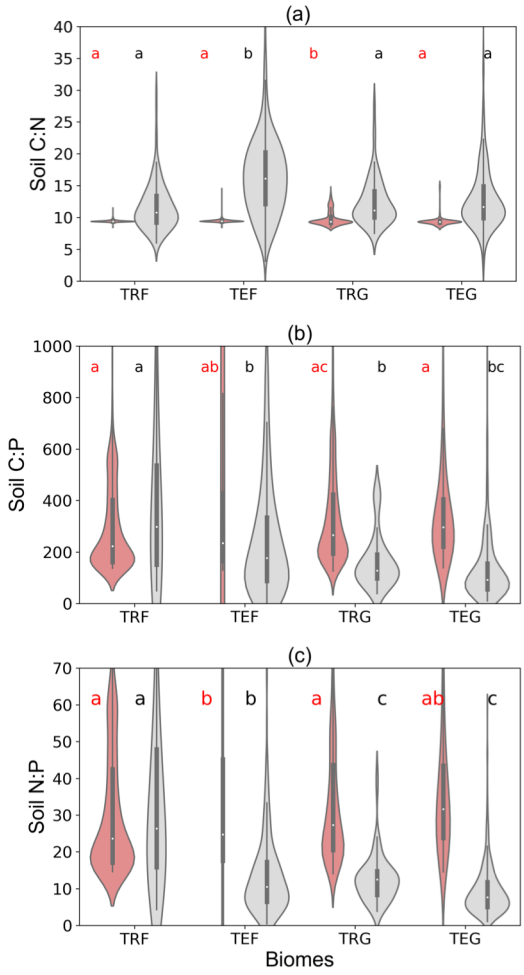

Figure 9: C:N, C:P and N:P ratios of soil organic matter by ORCHIDEE-CNP and plot-level measurements by Tipping et al. (2016) for 4 biomes: tropical forest (TRF), temperate forest (TEF), tropical grass (TRG) and temperate grass (TEG). Soil C:N:P ratios for ORCHIDEE-CNP are calculated for total soil pool includes soil passive, slow and active pools, while measurements by Tipping et al. (2016) are for soils of 0-60 cm depth. Alphabet 'a', 'b' and 'c' indicate the significance of differences among biomes from the analysis of variance (ANOVA).

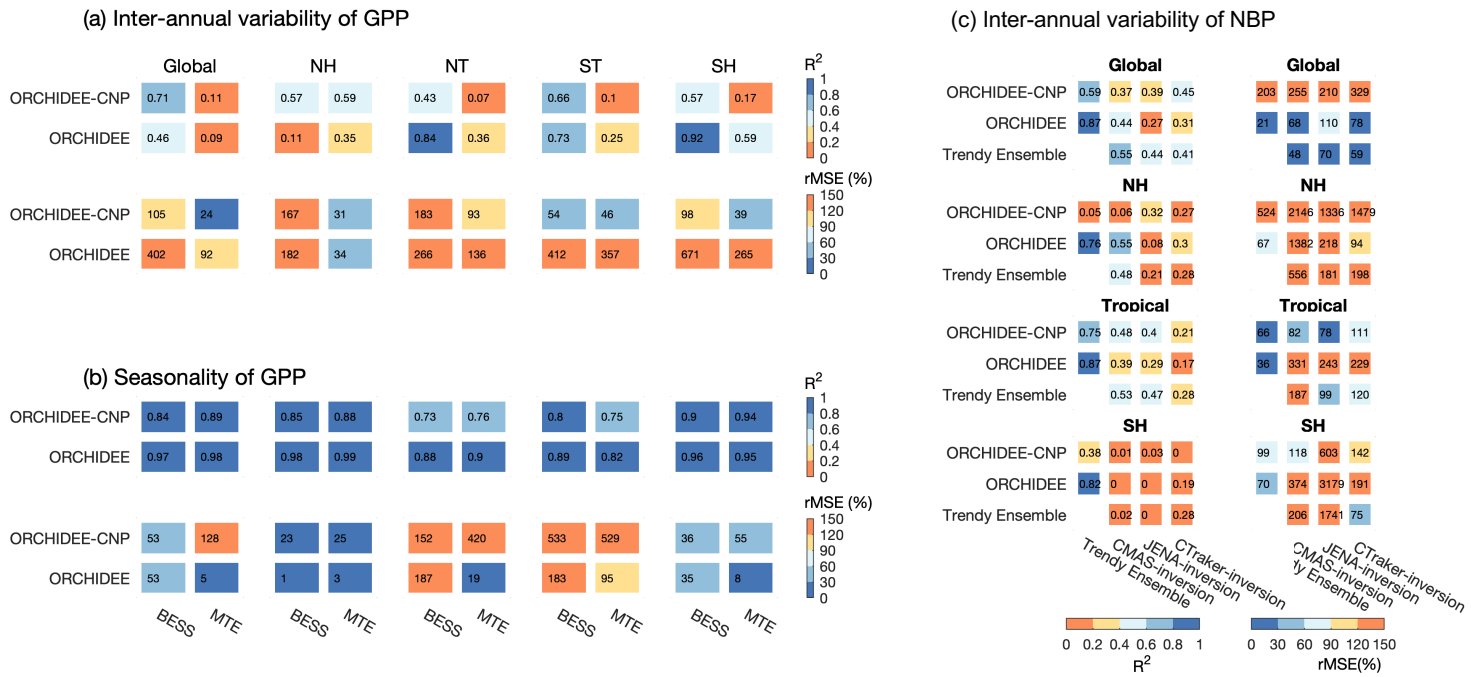

Figure 10: The performances of ORCHIDEE and ORCHIDEE-CNP on the inter-annual variability of de-trended anomalies of GPP during 2001-2010 (a), the seasonal variability of mean GPP across 2001-2010 (b) and the inter-annual variability of net biome productivity (NBP) (c). Two statistics were used to represent the model performance: coefficient of determination (R^2) and relative mean-square deviation (rMSE). For (a) and (b), the evaluations are for globe, the northern hemisphere (30°N-90°N; NH), north tropical (0°-30°N; NT), south tropical (0°-30°S; ST) and the southern hemisphere (30°S-90°S; SH). Two sets of observation-based GPP products BESS-GPP, MTE-GPP were used for the comparison. For (c), the evaluations are for globe, the northern hemisphere (30°N-90°N, NH), tropical (30°S-30°N), and the southern hemisphere (30°S-90°S; SH). Mean value across Trendy ensemble models (v6) and three sets of NBP from inversion datasets were used as the reference databases for the comparison with different available periods (Trendy Ensemble: 1959-2016; CAMS:1979-2016; JENA:1985-2016; CTracker: 2001-2016).